CREWES

Research Report 2019
Volume 31

In this volume…

Report Summaries

*For **Complete Reports** and **Student Theses** please visit:*

https://www.crewes.org

(Sign in/password required)

Reports

Theses

UNIVERSITY OF CALGARY
FACULTY OF SCIENCE
Department of Geoscience

Notice of Intent to Publish

Please note that the authors of the research in this 31st Volume of the Abstract Book intend to publish or otherwise publically disseminate their full research papers in the coming calendar year. According to the contracts between the University of Calgary (CREWES) and each Sponsor, the University will make available to the Sponsor a copy of the proposed publication resulting from the CREWES Project prior to submission for publication. In the event that the Sponsor determines that Research Results within the proposed publication contain Sponsor Confidential Information, the Sponsor shall have thirty (30) days to notify the University in writing and the University shall remove Sponsor Confidential information prior to publication. This 30 day period shall be considered to have started at the end of this meeting (December 11, 2019). These full research reports are available on the CREWES website to all Sponsors and their employees.

In memory of:

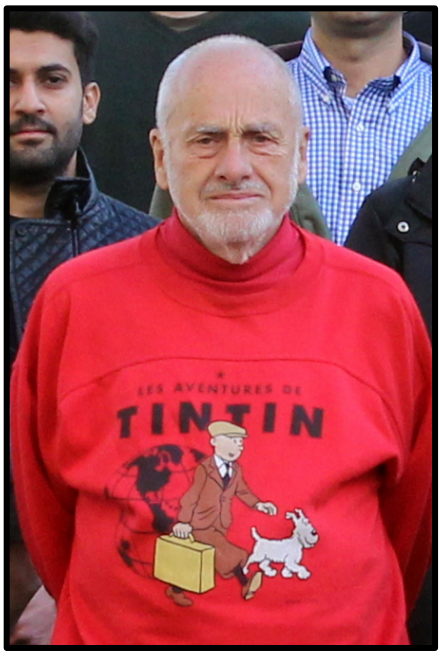

Claude Ribordy

1937-2019

It is with great fondness that we remember Claude Ribordy, who recently passed away after a short illness at the age of 82. In 2017, Claude retired from Hampson-Russell, now a subsidiary of CGG, and became a research assistant in the CREWES consortium at the University of Calgary. Remembering his quantum mechanics studies at university, Claude had recently become very interested in quantum computing, and was reading extensively about the subject. For Claude, there was always something new and exciting to learn. We all remember Claude's twinkling smile and the colourful red sweaters that he wore each year for the CREWES photograph (sometimes bearing the image of his favourite character, Tintin!).

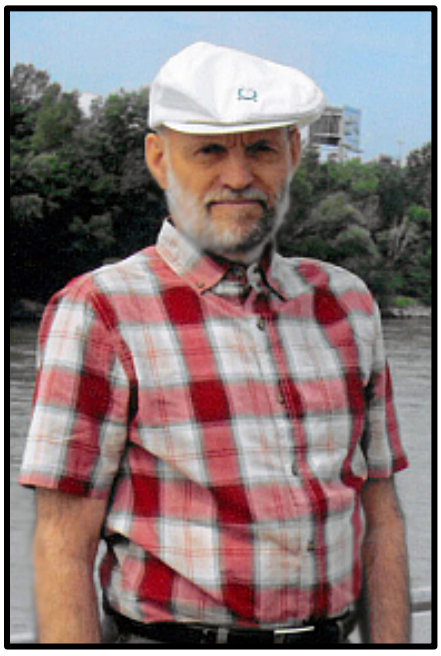

Arnim Haase

1941-2019

Arnim Haase was a staff member at CREWES for several years, after his retirement from a geophysical career in industry. He brought a focussed engineering outlook to everything he did professionally, always attempting to understand a problem fully before beginning his own work, usually starting from basic physical or mathematical principles. Arnim was unfailingly cheerful and outgoing, even as he struggled with his health; and we all remember him coming to the office every day dressed immaculately in a three-piece suit. He loved flying his own superlight aircraft, and he was always willing to vigorously debate the merits of political systems, based on his own early experiences behind the Iron Curtain, and his subsequent dramatic escape to the west.

CREWES in 2019

I'm pleased and delighted to welcome you to the CREWES Annual Sponsor's Meeting and technical review. The year 2019 was a signal one for us, with the students and researchers making big strides as they progressed their degree programs and research projects. This year, as the leadership was working to put together the technical program, I was once again struck by the breadth and depth of the research this group is carrying out. In these pages you'll find new ideas, data, and methods; steps forward in acquisition, processing, imaging and inversion – along with, I believe, a compelling case that they are not independent of one another, but parts of an integrated program of seismic research.

In 2019 we have progressed analysis of our large 2018 multi-azimuth / multi-offset VSP experiment, which we carried out in collaboration with CaMI-FRS, INOVA, Fotech, and later Halliburton. We have carried out basic processing of that large dataset, and we have begun setting out FWI methodologies prepared for DAS data as input. We are now reporting on calibration of the the multicomponent DAS fibre loop with the simultaneous 3C geophone data. New DAS modelling, multiple prediction, and surface wave inversion through both FWI and global approaches are all described. FWI for high resolution reservoir properties – is also a big subject this year: approaches to time lapse methods, direct updating of rock physics properties, FWI for DAS data, and new approaches to QC'ing FWI outputs have all been advanced. Theory guided machine learning offers not only an environment to implement and extend waveform inversion, interpolation, imaging, and deblending, but does so using architectures which fit naturally into cloud computing.

Two longstanding CREWES faculty have retired from the University of Calgary in 2019: Don Lawton and Larry Lines. We hope you will join us in wishing them fantastic retirements. The blow is not as bad as it seems, as we expect to continue working closely with both of them on ongoing research.

This year we lost Claude Ribordy and Arnim Haase, two gentlemen who made large contributions to our group over the years, and are sorely missed. I hope you'll take a moment to check out the memorial words to these gentlemen in this book.

All our efforts at CREWES rely critically on your continued support and the support of your companies. We greatly appreciate your role as the champions of CREWES within your companies and institutions, and for communicating what we do. We look forward to pushing our research and training forward in 2020 and beyond!

Calgary, Alberta
November, 2019

Kristopher Innanen
CREWES Director

Remembering Larry Lines
by Bernhard Mayer (U of C geoscience head) and Don Lawton, November 26, 2019

It is with profound sadness, that we share the news that our dear colleague Larry Lines passed away last night after a short illness.

Larry joined the Department of Geology & Geophysics in 1997 after receiving degrees from the University of Alberta (BSc) and UBC (PhD), after 17 years in industry with Amoco, and after a stint as Research Chair at Memorial University (St. John's, Newfoundland). Throughout his career, he published more than 50 peer-reviewed journal papers and hundreds of refereed conference contributions that are frequently cited in the academic community and widely utilized by industry practitioners. From 1997 to 2002, Larry held the CSEG Chair in Exploration Geophysics at the University of Calgary. Furthermore, he served as Director of the research consortium CHORUS and was Associate Director of CREWES and the Fold-Fault Research Project (FRP) and co-generated several million dollars in research funds. From 2002 to 2007, Larry was head of the Department of Geology & Geophysics. During his tenure at the University of Calgary, he instructed six different undergraduate courses in two different departments and taught four different graduate courses. He supervised or co-supervised a highly impressive number of 73 (!) graduate students. This is clear evidence that Larry has made tremendous contributions to research, teaching, mentoring and service in the Department of Geoscience and the Faculty of Science and to fostering the international reputation of the Geophysics program at the University of Calgary.

Of equal importance are Larry's outstanding research collaborations with industry partners through various industrial consortia and his leadership roles in professional societies. His numerous conference presentations and publications ensured that new academic knowledge was rapidly taken up in practical applications in industry. This activity also ensured that the Department of Geoscience remained well connected with industrial leaders in the community,

and with the companies that provided employment for countless Geoscience undergraduate and graduate students. Larry also had an exemplary record of service to his scientific discipline Exploration Seismology. For example, he served as both Editor and President of the Society of Exploration Geophysicists and as co-editor of the Canadian Journal of Exploration Geophysics, among various other appointments. In recognition of his extraordinary services he received many awards and honours including the Society of Exploration Geophysicists (SEG) Presidential Award and the Canadian Society of Exploration Geophysicists (CSEG) medal in 2017. This is clear evidence that Larry has made tremendous research and teaching contributions over more than two decades at this institution, and that he provided dedicated services on and off campus throughout his tenure at the University of Calgary.

And of most importance to us, Larry was a tremendous academic citizen, a great human being and friend, and a truly kind man. We cannot remember a single occasion where Larry was asked to take on a duty or task, where he would not have said with a happy face "yes of course, I would be glad to take on this responsibility"!

Larry will be sadly missed, and our deepest condolences go out to Larry's family, his colleagues, students and friends.

Table of Contents

* Oral Presenter

2019 CREWES Sponsors

Acceleware	CGG
Chevron Corporation	CNOOC International
Devon Energy Corporation	Halliburton
INOVA Geophysical	Petrobras
Petronas Carigali SDN BHD	Repsol Oil & Gas Canada Inc.
RIPED, PetroChina	Saudi Aramco
Sinopec	TGS

Natural Sciences and Engineering Research Council of Canada (NSERC) - Collaborative Research and Development Grant

NSERC CRSNG

Additional funding provided by:

CANADA FIRST RESEARCH EXCELLENCE FUND

MITACS

CREWES Personnel 2019

LEADERSHIP

Kristopher A. Innanen, Director
Professor, Department of Geoscience, University of Calgary

B.Sc. Physics and Earth Science, 1996, York University
M.Sc. Physics, 1998, York University
Ph.D. Geophysics, 2003, University of British Columbia

- Work Experience: University of Houston

Don C. Lawton, Associate Director
Director for Containment and Monitoring Institute (CaMI)

Faculty Professor, Department of Geoscience, University of Calgary

B.Sc. (Hons. Class I) Geology, 1973, University of Auckland
Ph.D. Geophysics, 1979, University of Auckland

- Work Experience: New Zealand Steel Mining Ltd., Amoco Minerals (N.Z.) Ltd., Carbon Management Canada

Daniel Trad, Associate Director
Associate Professor, Department of Geoscience, University of Calgary

Licenciatura in Geophysics, 1994, Universidad Nacional de San Juan, Argentina
Ph.D Geophysics, 2001, University of British Columbia

- Work Experience: Electromagnetic Methods (Argentina and Brazil), Seismic Research and development (Veritas, CGG, Techco, in Calgary and France)

Michael P. Lamoureux
Professor, Department of Mathematics and Statistics, University of Calgary

Adjunct Professor, Department of Geoscience, University of Calgary

B.Sc. Mathematics, 1982, University of Alberta
M.Sc. Mathematics, 1983, Stanford University
Ph.D. Mathematics, 1988, University of California, Berkeley

- Work Experience: Farallon Computing, NSERC Canada

Kevin W. Hall, Technical Manager

B.Sc. Geophysics, 1992, University of Calgary
M.Sc. Geophysics, 1996, University of Calgary

- Work Experience: Lithoprobe Seismic Processing Facility at the University of Calgary

Gary F. Margrave, Emeritus Director
Emeritus Professor, Faculty Professor, Department of Geoscience, University of Calgary

B.Sc. Physics, 1975, University of Utah
M.Sc. Physics, 1977, University of Utah
Ph.D. Geophysics, 1981, University of Alberta

- Work Experience: Chevron Canada Resources, Chevron Geoscience Company, Devon Canada, TGS Canada

Laurence R. Lines, Emeritus Director
Professor, Department of Geoscience, University of Calgary

B.Sc. Physics, 1971, University of Alberta
M.Sc. Geophysics, 1973, University of Alberta
Ph.D. Geophysics, 1976, University of B.C.

- Work Experience: Amoco Production Research, Tulsa University, Memorial University of Newfoundland

RESEARCH STAFF, POST DOCS AND VISITING SCHOLARS

Amr Ibrahim

B.Sc. Physics, 2003, Cairo University, Egypt
M.Sc. Physics 2008, Beni Suef University, Egypt
M.Sc. Physics, 2010, University of Lethbridge, Canada
PhD, Geophysics, 2015, University of Alberta

- Work Experience: Lecturer, Physics Department at Beni Suef University, Egypt, Post Doctoral Fellow at the Center for Subsurface Imaging and Modelling (CSIM), King Abdullah University of Science and Technology (KAUST), Saudia Arabia.

Kevin L. Bertram

Electronics Technician Certificate, 2005, Southern Alberta Institute of Technology

- Work Experience: Aram Systems Ltd.

Malcolm B. Bertram

B.Sc. Geology, Auckland, New Zealand

- Work Experience: GSI (Western Australia), Western Geophysics (Western Australia), Auckland University, University of Calgary

Raúl Cova

B.Sc. Geophysical Engineering, 2004. Simon Bolivar University, Venezuela
Ph.D. Geopysics, 2017, University of Calgary
Graduate Diploma in Petroleum Studies, 2011, IFP School, Venezuela

- Work experience: PDVSA Intevep. Venezuela, Shell Canada

Ali Fathalian

B.Sc. Applied Physics, 2001, University of Razi, Iran
M.Sc. Condensed Matter Physics, 2003, University of Razi, Iran
Ph.D. Condensed Matter Physics, 2007, University of Razi, Iran
Ph.D. Geophysics, 2019, University of Calgary

Marcelo Guarido de Andrade

B.Sc. Physics, 2006, University of São Paulo, Brazil
M.Sc. Geophysics, 2008, University of São Paulo, Brazil
Ph.D. Geophysics, 2017, University of Calgary

- Work Experience: Verdazo Analytics, Schlumberger (Houston), PGS (Rio de Janeiro, Brazil), Orthogonal Geophysics, Husky Energy

David C. Henley

B.Sc. Physics, 1967, Colorado State University
M.Sc. Physics, 1968, University of Michigan

- Work Experience: Shell Oil Co., Shell Canada Ltd.

Helen Isaac

B.Sc. Mathematics, 1973, Imperial College, London
M.Sc. Geophysics, 1974, Imperial College, London
Ph.D. Geophysics, 1996, University of Calgary

- Work Experience: Phillips Petroleum Company, Hudson's Bay Oil and Gas, Canterra Energy, Husky, Fold-Fault Research Project at the University of Calgary

Marie Macquet

B.Sc. Earth Science, 2009, University of Nantes (France)
M.Sc. Planetology, 2011, University of Nantes (France)
Ph.D. Geophysics, 2014, Isterre, University of Grenoble (France)

Nasser Kazemi Nojadeh

B.Sc. Geology, 2007, University of Tabriz
M.Sc. Geophysics, 2010, University of Tehran
Ph.D. Geophysics, 2017, University of Alberta

- Work Experience: Statoil ASA Research Group, Norway

Hongliang Zhang

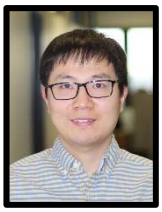

B.Sc. Geophysics, 2010, China University of Geosciences, Wuhan, China
M.Sc. Petroleum Geology, 2013, Peking University, Beijing, China
Ph.D. Geophysics, 2019, University of Calgary

- Work Experience: Institute of Geology and Geophysics, Chinese Academy of Sciences, Beijing, China

GRADUATE STUDENTS

Hussain Aldhaw

B.Sc. Geosciences, 2012, University of Tulsa, Oklahoma

- Work Experience: Saudi Aramco

Ninoska Amundaray

B.Sc. Geophysical Engineering, 2016, Simon Bolivar University, Venezuela

- Work experience: PDVSA, Venezuela

Farzaneh Bayati

B.Sc. Physics, 2008, University of Science and Technology
M.Sc. Geophysics Exploration, 2012, University of Tehran

- Work experience: Tehran Energy Consultants company (TEC), Tehran, Iran

Matt Eaid

B.Sc. (First Class Honours) Geophysics, 2015, University of Calgary

- Work experience: Shell Canada Ltd., Husky Energy, Chevron Energy Technology Company

Xin Fu

B.Sc. Geophysics, 2015, China University of Petroleum (East China)
M.Sc. Geophysics, 2018, China University of Petroleum(Beijing)

Heather Hardeman-Vooys

B.Sc. Mathematics (summa cum laude), 2012, University of Montevallo, AL, USA
M.A. Mathematics, 2014, Wake Forest University, NC, USA.

- Work Experience: Fotech Solutions

Qi Hu

B.Sc. Geophysics, 2011, Yangtze University, Hubei, China
M.Sc. Geophysics, 2014, China University of Petroleum, China

- Work Experience: Sinopec Geophysical Research Institute

Shang Huang

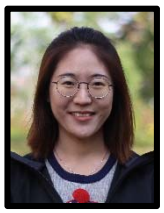

B.Eng. Geophysics, 2017, China University of Petroleum, China
M.Sc. Geophysics, 2018, University of Calgary

Andy Iverson

B.Sc. Geophysics (First Class Honours), 2012, University of Calgary

- Work Experience: Apache Canada Ltd, Nexen Energy ULC, Velvet Energy Ltd.

Scott Keating

B.Sc. with Honours in Physics 2014, University of Alberta

- Work Experience: CNOOC International

Brendan Kolkman-Quinn

B.Sc. with Honours in Physics, 2009, University of Alberta
B.Sc. Geophysics, 2014, University of Calgary

- Work Experience: ConocoPhillips Canada

Bernie Law

B.Sc. Geological Engineering (Geophysics), 1982, University of Saskatchewan

- Work Experience: Key Seismic Solutions Ltd., Precision Seismic, Veritas Software, SDP

Arthur Lee

B.Sc. in Electrical Engineering (minor in Computer Engineering), 1988, University of Calgary

- Work Experience: Hampson-Russell GeoSoftware CGG Calgary

Da Li

B.Sc. Geophysics, 2012, China University of Geosciences (Beijing)

M.Sc. Geophysics, 2016, China University of Geosciences (Beijing)

He Liu

B.Sc. Prospecting Technology and Engineering, 2012, China University of Petroleum (Beijing)

M.Sc. Geophysics, 2014, China University of Petroleum (Beijing)

Ph.D. Geophysics, 2019, China University of Petroleum (Beijing)

Ellen Liu

B.Sc. Chemical Engineering, 2014, University of Alberta

- Work Experience: ConocoPhillips Canada

Jorge Monsegny

B.Sc. Computer Science, 2003, National University of Colombia

M.Sc. Mathematics, 2007, National University of Colombia

- Work Experience: Santander Industrial University, Ecopetrol ICP, National University of Colombia

Zhan Niu

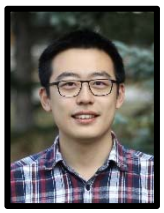

B.Sc. Geophysics (First Class Honours with minor in geology), 2017, University of Calgary

Luping Qu

B.Sc. Geophysics, 2014, China University of Petroleum (East China)

M.Sc. Geophysics, 2017, China University of Petroleum (Beijing)

Ziguang Su

B.Eng. Exploration Geophysics, 2017, China University of Petroleum, China
B.A. English, 2017, China University of Petroleum
M.Sc. Geophysics, 2018, University of Calgary

Ron Weir

B.Sc. Geophysics, 1978, University of Alberta
- Work Experience: Harvest Operations Corp/KNOC

Tianze Zhang

B.Sc. Applied Geophysics, 2015, Jilin University, China
M.Sc. Geological Engineering, 2018, Jilin University, China

Kai Zhuang

B.Sc. Geophysics, 2018, University of Calgary

ASSOCIATED FACULTY and SCIENTISTS

Huaizhen Chen
Research Fellow, Tongji University, Shanghai, China
Adjunct Researcher, CREWES, University of Calgary

Ph.D. Geophysics, 2015, China University of Petroleum
B.Sc. Geophysics, 2010, China University of Petroleum

Andreas Cordsen
Technical Advisor, CREWES, University of Calgary

M.Sc. Geology, 1975, Queen's University, Kingston
M.Sc. Geophysics, 1980, Dalhousie University, Halifax
- Work Experience: BEB, Esso Resources, Norcen Energy, GEDCO, Schlumberger, CHAD Data Ltd.
-

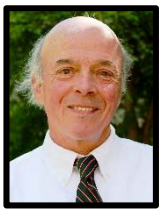

Sam Gray
Technical Advisor, CREWES, University of Calgary

B.S. Math, 1970, Georgetown University
Ph.D. Math, 1978, University of Denver
- Work experience: U.S. Naval Research Lab, General Motors Institute, Amoco, BP, Veritas, CGG

Rachel Lauer
Assistant Professor, University of Calgary

B.Sc. Psychology, Bryn Mawr College
M.Sc. Environmental Engineering Geoscience, Radford University
Ph.D. Geoscience, Pennsylvania State University

- Work Experience: Consultant at NAEVA Geophysics

Faranak Mahmoudian
Technical Advisor, CREWES, University of Calgary

B.Sc. Applied Physics, 2000, K. N. Toosi University of Technology, Iran
M.Sc. Geophysics, 2006, University of Calgary
Ph.D. Geophysics, 2013, University of Calgary

- Work Experience: Shell Canada, Earth Signal Processing

Brian H. Russell
Adjunct Professor, Department of Geoscience, University of Calgary

B.Sc. Physics, 1972, University of Saskatchewan
Honours Certificate in Geophysics, 1975, University of Saskatchewan
M.Sc. Geophysics, 1978, University of Durham
Ph.D. Geophysics, 2004, University of Calgary

- Work Experience: Chevron Geoscience Company, Teknica Resource Development, Veritas Software Ltd., Hampson-Russell Software Ltd, CGG GeoSoftware

Roman Shor
Assistant Professor, Department of Chemical and Petroleum Engineering, University of Calgary

Associate Head (Undergraduate Studies), Department of Chemical and Petroleum Engineering, University of Calgary

B.Sc. Computer Science, 2009, University of Pennsylvania
M.Sc. Computer Science, 2010, University of Pennsylvania
M.Sc. Petroleum Engineering, 2014, University of Texas at Austin
Ph.D. Petroleum Engineering, 2016, University of Texas at Austin

- Work Experience: Shell, Merck, Lehman Brothers

Robert R. Stewart
Cullen Chair in Exploration Geophysics, University of Houston

Adjunct Professor, Department of Geoscience, University of Calgary

B.Sc. Physics and Mathematics, 1978, University of Toronto
Ph.D. Geophysics, 1983, Massachusetts Institute of Technology

- Work Experience: Veritas Software Ltd., Gennix Technology Corp., University of Calgary

Xiucheng Wei
Technical Advisor, CREWES, University of Calgary

B.Sc. Geophysics, 1982, China University of Petroleum
M.Sc. Geophysics, 1992, China University of Petroleum
Ph.D. Geophysics, 1995, China University of Petroleum

- Work Experience: China National Petroleum Company (CNPC), China University of Petroleum (CUP), British Geological Survey (BGS), China Petroleum & Chemical Corporation (Sinopec), International Research Coordinator with the Faculty of Science at the University of Calgary

Joe Wong

B.Sc. Physics/Mathematics, 1971, Queen's University
M.Sc. Applied Geophysics, 1973, University of Toronto
Ph.D. Applied Geophysics, 1979, University of Toronto

- Work Experience: Ontario Ministry of the Environment, University of Toronto, JODEX Applied Geoscience Limited, CREWES

Matt Yedlin
Associate Professor, Department of Electrical and Computer Engineering, University of British Columbia

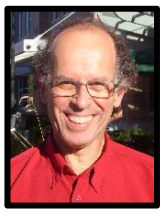

B.Sc. Honours Physics, 1971, University of Alberta
M.Sc. Physiology, 1973, University of Toronto
Ph.D. Geophysics, 1978, University of British Columbia

- Work Experience: Conoco

Student Theses

The following theses were completed with CREWES in 2019:

M.Sc.	Hussain Aldhaw	Processing of Multicomponent Seismic Data from West-Central Alberta
M.Sc.	Timothy Alan Cary	Time-lapse Electrical Resistivity Imaging of Methane Gas Migration in a Shallow Confined Aquifer
Ph.D.	Ali Fathalian	Anelastic Attenuation and Anisotropy in Seismic Data: Modeling and Imaging
M.Sc.	Adriana Josefina Gordon Ferrebus	Processing of DAS and geophone VSP data from the CaMI Field Research Station
Ph.D.	Heather Hardeman-Vooys	Event detection and classification using distributed acoustic sensors
M.Sc.	Lei Yang	Comparisons and Implementations of Least-squares Reverse Time Migration and Full Waveform Inversion in Acoustic Media

NOTES

Exploring two different methods of seismic interpolating operators

Farzaneh Bayati and Daniel Trad

ABSTRACT

3D land data acquisitions are often undersampled along offset and azimuth directions because of large shot and receiver line intervals. In marine data acquisition, data are well sampled in the inline direction but coarsely sampled in the crossline direction. These issues can often be alleviated by seismic interpolation, which is an important step in data processing since many processing and migration tools require regularly sampled input data.

We compare two methods of seismic amplitude reconstruction. The first one is singular spectrum analysis (SSA) which is based on rank reduction methods. In this approach, we generate Hankel matrices from constant frequency data and reduce their rank by using Truncated Singular Value Decomposition (TSVD). Since missing traces and random noise increase the rank of the Hankel matrix, TSVD changes the data by removing noise and interpolating missing traces. By reducing the rank, the algorithm iteratively infills missing traces. The second method is Minimum Weighted Norm Interpolation (MWNI) which infills missing traces by transforming the data to the Fourier domain and removing sampling artifacts by enforcing wavenumber-domain sparsity.

In this report, we test how these two methods perform on pre-stack and irregular sampled synthetic 2D data. For the case we tested, SSA seems more affected by curvature than MWNI but it seems better in preserving the amplitude for the hyperbola flanks. For SSA, we implement a multidimensional version and test it for 3D synthetic data.

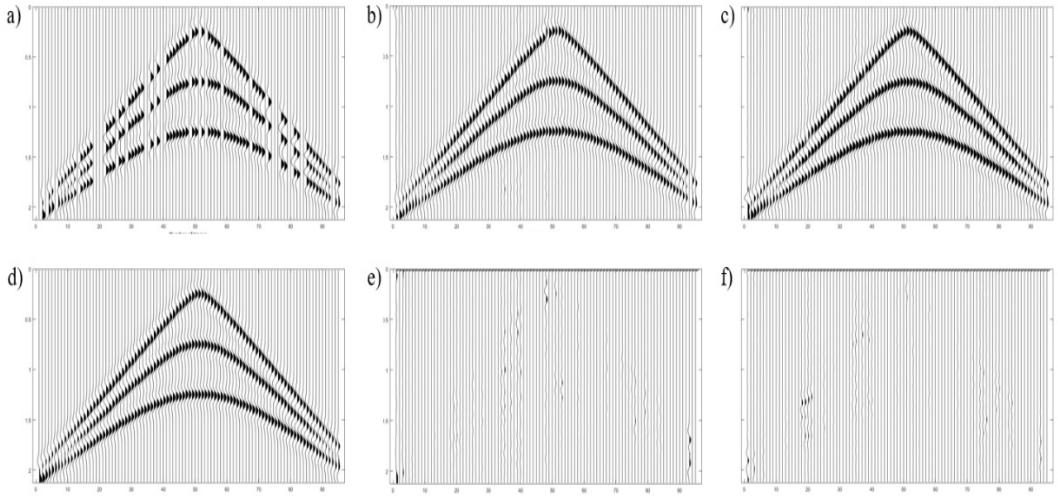

FIG. 1. Comparison between the singular spectrum analysis algorithm and minimum weighted norm interpolation algorithm applied to the 2-D pre-stack synthetic noiseless data having 3 different curved events and 30% decimated traces. a) Input data with 30% decimated traces; b) result of applying the singular spectrum analysis algorithm; c) result of applying the minimum weighted norm interpolation algorithm; d) expected data; e) difference between (b) and (d); f) difference between (c) and (d).

CREWES in the field: 2019 overview

Kevin L. Bertram*, Kris Innanen, Kevin W. Hall, Marie Macquet, Malcolm Bertram, and Don C. Lawton

ABSTRACT

Simulated data is useful for testing various processing methods, but there is still a huge advantage to using data acquired in the "real world". CREWES has a long history of acquiring and processing field data. With access to several different acquisition tools and instruments several different experiments can be carried out. This year fieldwork acquisition was exclusively done at the CaMI FRS.

Projects that CREWES has been involved with this year include: a) the setup of several passive monitoring three component recording stations; b) an acquisition experiment with a repeatable source location before, during, and after carbon dioxide injection into an underground reservoir; c) the 2019 Geophysics Undergraduate Field School with the University of Calgary's Geoscience Department; d) the setup of repeatable source locations for a walk-away/walk-around VSP.

FIG. 1. Equipment and data in the field.

Inversion for two sets of fracture weaknesses using differences between azimuthal reflection coefficients

Huaizhen Chen, Junxiao Li, and Kris Innanen

ABSTRACT

We first express stiffness parameters in terms of two sets of fracture weaknesses for the case of fractured rock consisting of two orthogonal sets of vertical fractures. Using perturbations in these stiffness parameters for the case of an interface separating an isotropic layer and a fractured layer, we derive a linearized P-to-P reflection coefficient as a function of two sets of fracture weakness, and we present differences in azimuthal reflection coefficients in terms of the tangential fracture weaknesses and the normal fracture weakness intercepts. Using the differences in azimuthal reflection coefficients, we establish an approach of estimating the tangential fracture weaknesses and the normal fracture weakness intercepts following a Bayesian framework. Synthetic tests confirm that the unknown parameter vector involving the tangential fracture weaknesses and the normal fracture weakness intercepts is estimated stably and reliably in the case of signal-to-noise ratio of 2.

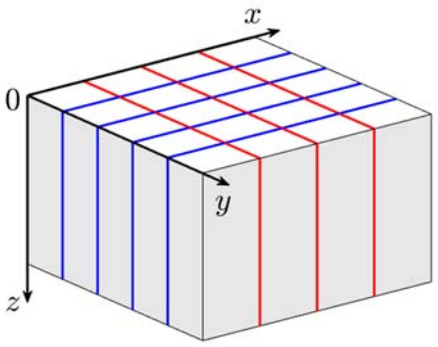

FIG. 1. A model of fractured rock consisting of two orthogonal sets of vertical fractures.

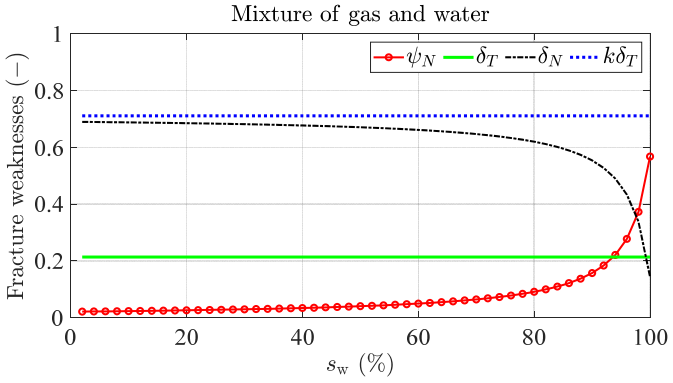

FIG. 2. Variations of fracture weaknesses (δ_N, δ_T) and normal fracture weakness intercept (ψ_N) with water saturation.

Joint inversion of PP- and PSV-wave amplitude data for estimating P- and S-wave moduli and attenuation factor

Huaizhen Chen, Shahpoor Moradi, and Kris Innanen

ABSTRACT

Beginning with re-expressing P- and S-wave velocities in anelastic media, we first propose frequency-dependent P- and S-wave moduli in terms of P- and S-wave moduli at a reference frequency and P-wave maximum attenuation factor, in which we replace S-wave attenuation factor with P-wave maximum attenuation factor. Based on Zoeppritz equations and their linearized expressions for computing PP and PSV-wave reflection coefficients, we derive frequency-component PP- and PSV-wave reflection coefficients as a function of P-wave maximum attenuation factor, from which anelastic impedances for PP- and PSV waves are expressed. Using the derived reflection coefficients and elastic impedances, we establish a two-step inversion approach, which involves the estimation of attenuative PP- and PSV-wave anelastic impedances from frequency-components of partially-stacked seismic data, and the prediction of unknow parameter vector (P- and S-wave moduli, density and P-wave maximum attenuation factor) using the estimated PP- and PSV-wave anelastic impedances. Synthetic tests confirm that the unknown parameters are estimated stably and reliably in the case of seismic data containing a moderate Gaussian noise. Applying the inversion approach to a real data set acquired over an oil-bearing reservoir, we observe reasonable results of P-wave maximum attenuation factor are obtained, which may provide additional proofs for fluid identification.

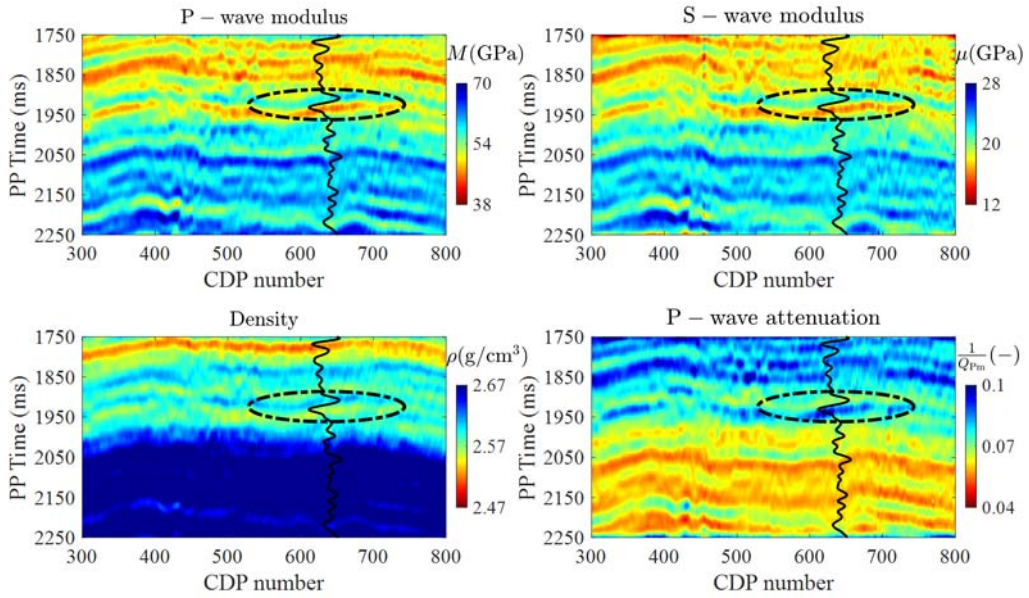

FIG. 1. Inversion results of P- and S-wave moduli, density and P-wave maximum attenuation factor.

Nonlinear inversion of seismic amplitude data for attenuation and layer-weaknesses

Huaizhen Chen and Kris Innanen

ABSTRACT

Based on a model of periodically layered media, we first express frequency-dependent stiffness parameters in terms of P-wave attenuation factor and lay-weaknesses. Using perturbations in frequency-dependent stiffness parameters for an interface separating two periodically layered media, we derive a linearized P-to-P reflection coefficient as a function of layer-weaknesses and P-wave attenuation factor, from which an expression of anisotropic and anelastic impedance is proposed. In order to estimate layer-weaknesses and P-wave attenuation factor, we first utilize a model-based damped least-squares inversion approach to estimate the anisotropic and anelastic impedances from frequency-components of partially-stacked seismic data. Using the estimated anisotropic and anelastic impedances, we implement nonlinear inversion for unknow parameter vector (P- and S-wave moduli, density, layer-weaknesses and P-wave attenuation factor), in which Bayesian Markov chain Monte Carlo algorithm is employed. Synthetic tests confirm that the unknown parameter vector involving P- and S-wave moduli, density, layer-weaknesses and P-wave attenuation factor is estimated stably and reliably in the case of signal-to-noise ratio of 2. Applying the inversion approach to a field data set, we observe that reliable results of layer-weaknesses and P-wave attenuation factor are obtained. We conclude that the proposed inversion approach may provide additional proofs for reservoir characterization and fluid identification.

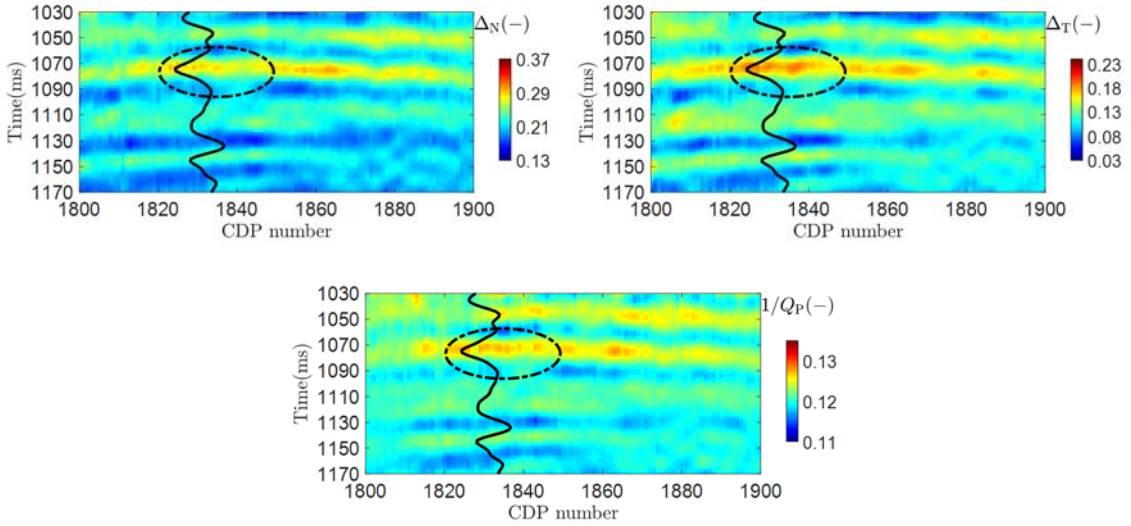

FIG. 1. Inversion results of layer-weaknesses and P-wave attenuation factor.

Full waveform inversion of multimode surface wave data: numerical insights

Raúl Cova* and Kris Innanen

ABSTRACT

Full waveform inversion has demonstrated to be a powerful tool for high resolution velocity model building. However, using surface wave data in FWI presents many challenges. In particular, the dispersive nature of surface waves results in the amplification of cycle skipping problems. Here, we propose decomposing surface waves in their fundamental and higher order modes and inverting them in a sequential approach to mitigate this problem. Even though the fundamental mode amplitudes are typically larger than the higher order modes, the latter ones can travel in the deeper parts of the near-surface at higher frequencies. Therefore, we use the fundamental mode to produce an initial approximation to the near-surface S-wave velocities and then perform another step of FWI using the higher modes to produce a more detailed velocity profile, particularly at larger depths. We also argue that although each individual higher mode is less energetic than the fundamental mode, as a group, the combination of all higher modes surpasses the energy and reach of the fundamental mode. We performed the modal separation by designing a mask in the F-K domain that roughly contains the energy of each mode. Results obtained from synthetic data demonstrate the potential of this approach to avoid cycle skipping and to improve the resolution of inverted S-wave velocity models.

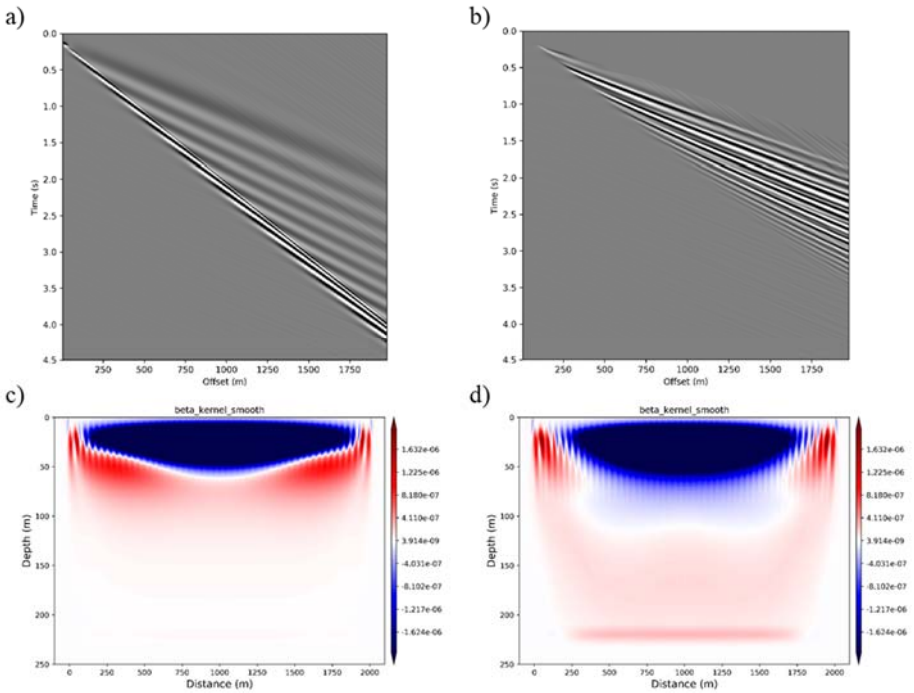

FIG. 1. Top: (a) Fundamental and (b) higher order surface wave modes after modal decomposition. Bottom: Vs model updates provided by (c) fundamental and (d) higher order modes data individually. Notice how the higher order modes provide a model update that reaches larger depths than the fundamental mode.

Coherent optical time domain reflectometry: the theoretical basis for distributed acoustic sensing technologies

Matt Eaid and Kris Innanen

ABSTRACT

The applications of distributed acoustic sensing (DAS) fibres for seismic acquisition, reservoir monitoring, and smart city applications continues to expand. As the interest in utilizing optical fibres for seismic acquisition continues to grow, it becomes increasingly important to understand the underlying technology that makes them effective. Understanding the theoretical means by which DAS fibres acquire seismic data allows for an improved understanding of their limitations and opportunities, and permits better decision making in how they are deployed. A grasp of the theory behind DAS technology also aids in the interpretation of the data, and trouble shooting when challenges arise. The way in which a given interrogator unit converts disturbances along the fibre to seismic strain varies and is typically proprietary. However, most implementations are based on a variant of coherent optical time domain reflectometry (COTDR), a technology used by telecommunications companies to detect flaws in installed optical fibres. In this short note we cover the topic of COTDR and discuss how it has been adapted for use in the acquisition of strain data resulting from seismic wave propagation.

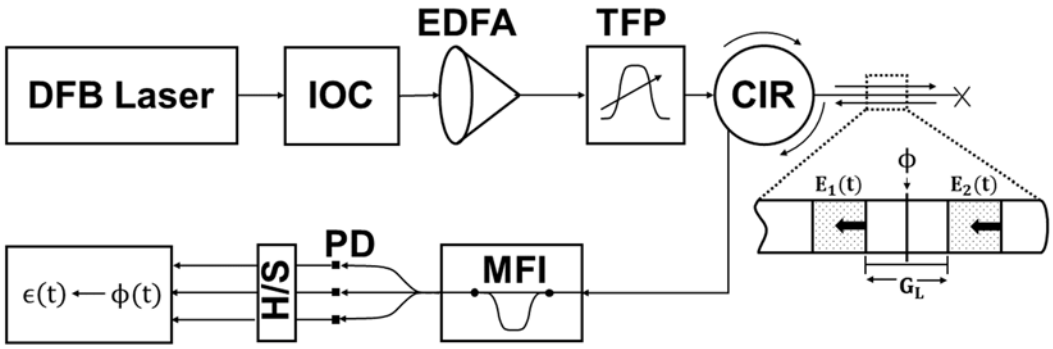

FIG. 1. Modern interrogator circuitry. The laser is modulated by an integrated optical chip (IOC), then amplified by an erbium doped amplifier (EDFA) and filtered for noise by a tunable Fabry-Perot filter (TFP). The pulse then enters an optical circulator (CIR) which transmits it to the fibre. The backscattered signal is delayed by the Mach-Zehnder interferometer (MZI) and split to three photo-diodes (PD). The signal is demodulated for the phase, which is empirically converted to strain. The return signal is then gated to analyze varying portions of the fibre. Modified from Posey Jr. et al. (2000).

Constructing meaningful FWI gradients for data from shaped DAS fibres

Matt Eaid*, Scott Keating, and Kris Innanen

ABSTRACT

Distributed acoustic sensing (DAS) has garnered significant interest as a seismic acquisition technology, especially in borehole deployments. A lingering question is how to best utilize DAS data to estimate reservoir properties. In contrast to geophones in conventional VSP surveys which measure three orthogonal components of particle velocity, DAS supplies a single measurement of tangential strain or strain rate along an optical fibre. Shaping DAS fibres increases the number of tangents they sample, and therefore the portion of the wavefield they sample. Elastic full waveform inversion is a robust means of estimating elastic subsurface parameters, however, it is conventionally formulated to incorporate particle velocity data supplied by geophones. We reformulate the conventional least-squares FWI objective function to incorporate the strain data supplied by distributed acoustic sensing fibres. The method developed in this paper can incorporate strain data from straight and shaped DAS fibres, and because it utilizes the conventional FWI formulation is capable of inverting data from geophones and DAS fibre simultaneously. We explore the effect that shaping DAS fibres has on the quality of parameter estimations from a toy model by comparing inversion results from a straight DAS fibre in a horizontal well and three helical fibres with varying wind rates. A simultaneous inversion of reflection geophone data and DAS data from horizontal well is examined and shown to provide enhanced parameter estimations over either dataset alone. FWI using DAS data is then tested on a portion of the Marmousi 2 model.

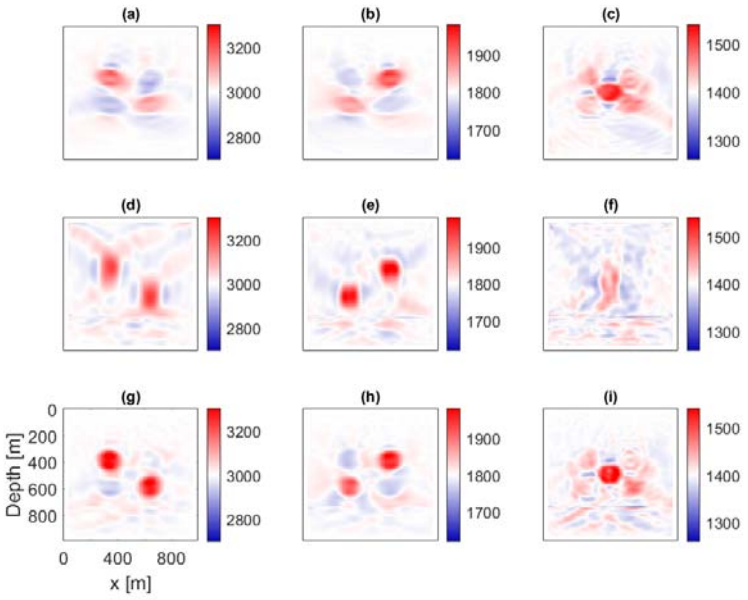

FIG. 1. Inversion results for v_p (column 1), v_s (column 2), and ρ (column 3) for reflection geophone data (a)-(c), strain data from a 1:4 helical fibre in a horizontal well (d)-(f), simultaneous inversion of reflection geophone data and strain data from a 1:4 helical fibre in horizontal well (g)-(i).

Modelling DAS signals for hydraulic fracturing and caprock monitoring

Matt Eaid* and Kris Innanen

ABSTRACT

Passive seismic technologies are indispensable tools for monitoring hydraulic fracture growth, caprock integrity during cyclic steam stimulation (CSS) and CO_2 sequestration, and borehole casing integrity. Mature fields use a combination of permanent arrays and temporary wireline tools to monitor the reservoir and optimize production. Conventionally, passive seismic monitoring consists of large arrays of surface and downhole geophones. This can result in the drilling of dedicated monitor wells, and well shut-in during wireline monitoring, resulting in elevated costs. Distributed acoustic sensing (DAS) uses non-invasive optical fibres that can be cemented behind casing in producing and injecting wells, offering an opportunity for the dual purposing of wells and reduced monitoring costs. DAS has the potential to be a powerful reservoir monitoring technology. To better understand the capabilities of DAS for reservoir monitoring, we develop an analytic modeling tool for DAS signals from moment tensor sources, providing data like that expected from hydraulic fracturing and CSS treatments. This tool provides an efficient means of examining DAS signals from various moment tensor sources. In this paper this tool is used to investigate the diagnostic characteristics in the DAS signals from different moment tensor sources and gain an enhanced understanding of the effect of source mechanics on DAS signals.

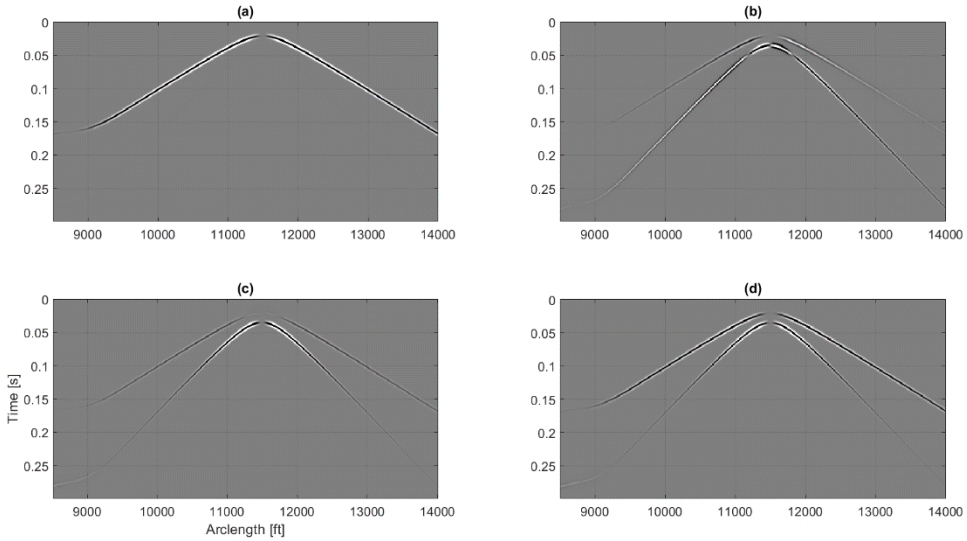

FIG. 1. Passive seismic shot records from a DAS fibre in horizontal well from an explosive source (a), double couple source (b), compensated linear vector dipole source (c), tensile crack opening type source (d). These shot records highlight the diagnostic characteristics contained in shot records from various moment tensor sources.

3D viscoacoustic reverse time migration with attenuation compensation

Ali Fathalian, Daniel Trad, and Kris Innanen

ABSTRACT

Processes of attenuation and dispersion always degrading the resolution of migrated images. To improve the image resolution, we have developed a new approach for the numerical solution of the 3D viscoacoustic wave equation in the time domain and we developed an associated reverse time migration (Q-RTM) method. The main feature of the Q-RTM approach is compensation of attenuation effects in seismic images during migration by separation of amplitude attenuation and phase dispersion terms. In the Q-RTM implementation, attenuation and dispersion compensated operators are constructed by reversing the sign of the amplitude attenuation and keeping the sign of dispersion operator unchanged. The Q-RTM approach is tested on a 3D model. We validate and examine the response of this approach by using it within an RTM scheme adjusted to compensate for attenuation. Our 3D numerical test focus on the amplitude recovery and resolution of the Q-RTM images as well as the interface locations. Numerical results show that the Q-RTM approach produced higher resolution images with recovered amplitude compared to the non-compensated RTM.

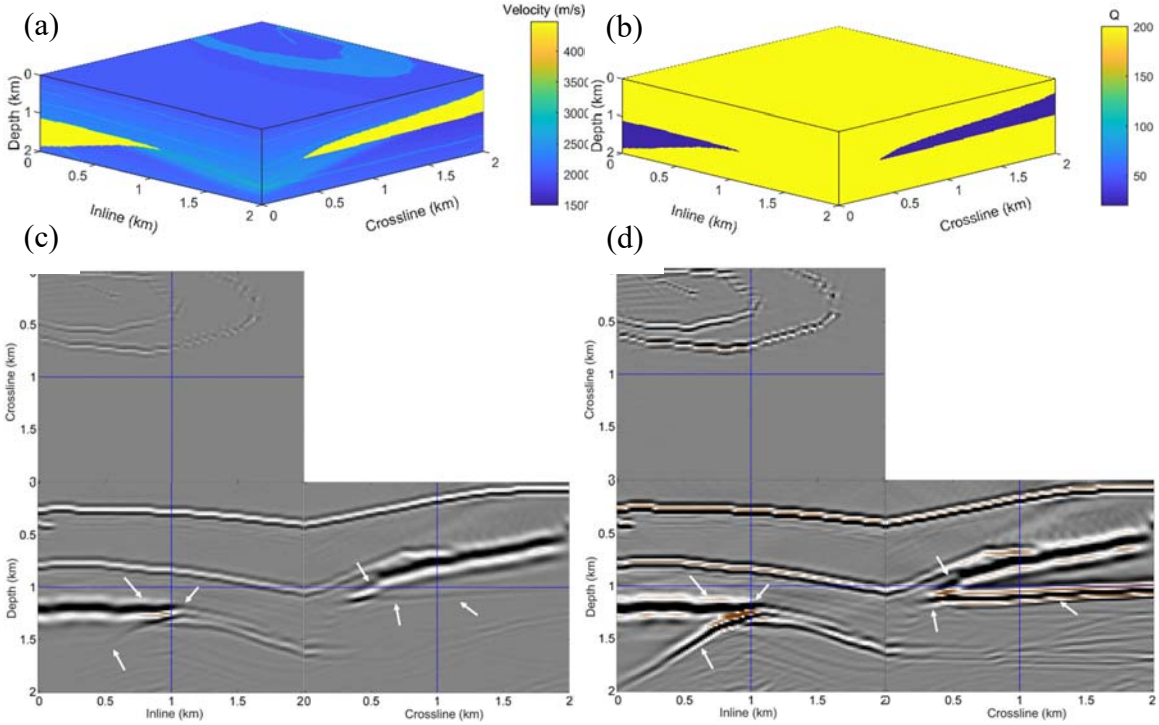

FIG. 1. (a) Velocity cubes in the 3D SEG/EAGE salt model, (b) Q model, (c) acoustic RTM image with viscoacoustic data (noncompensated). It is obvious the attenuation effect especially for Salt flanks under the high-attenuation zone., and (d) viscoacoustic RTM image (compensated). RTM image is clear, and the position is accurate from compensated viscoacoustic RTM.

Bayesian generalized linear AVA inversion for VTI media

Xin Fu and Kris Innanen

ABSTRACT

The research in this paper is to realize the simultaneous AVA (amplitude variation with angle) inversion of anisotropic parameters for the transversely isotropic media with vertical axis of symmetry (VTI media). First, we introduce a nonlinear PP-wave reflection coefficient approximation equation called ASI equation for isotropic elastic media. Then by replacing the isotropic part of Rüger equation with this equation, we obtain a new PP-wave reflection coefficient approximation equation called ASI Rüger equation for VTI media. In order to invert the VTI parameters based on ASI Rüger equation, we develop the Bayesian generalized linear inversion (BGLI), in which the noise and model perturbation are assumed to conform to the zero mean Gaussian distribution. ASI Rüger equation can express the PP-wave reflection coefficient in VTI media well. Compared with Rüger equation, ASI Rüger equation demonstrates less sensitivity to the bias in the intrinsic constant, lowers the relevance between the parameters, and reduces the ill-posedness of inversion problem. The synthetic data test shows that the proposed method can stably and reliably invert VTI parameters (the vertical P-wave impedance, the vertical S-wave impedance, Thomsen's parameters δ and ε), and the inverted results are almost unaffected by the errors in the intrinsic constant.

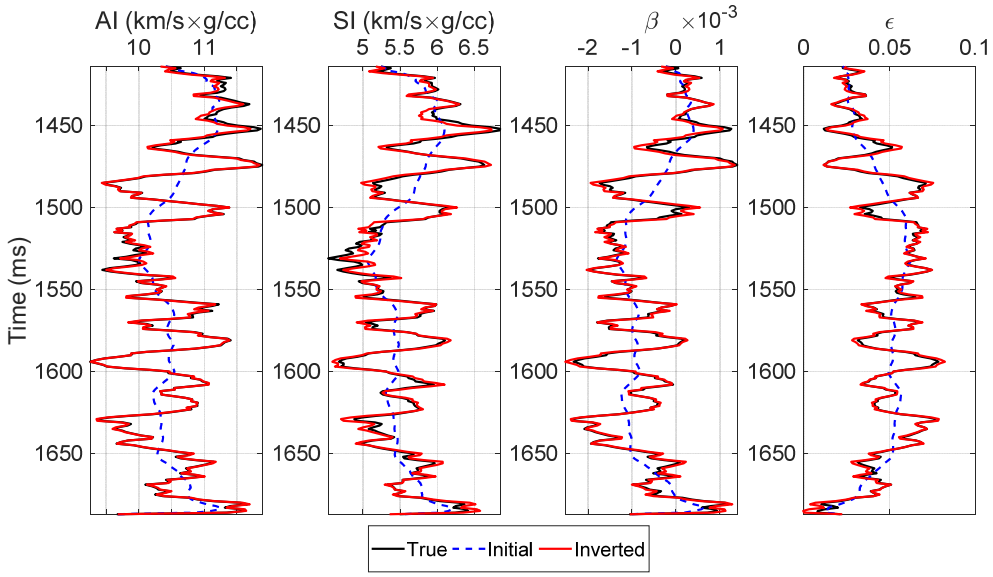

FIG. 1. The inverted results using synthetic data with the signal to noise ratio (SNR) 1:1.

Double-wavelet double-difference time-lapse waveform inversion

Xin Fu*, Sergio Romahn, and Kris Innanen

ABSTRACT

Time-lapse seismic data are widely used to monitor reservoir changes. And time-lapse waveform inversion is a valuable tool for seismic exploration. A popular time-lapse waveform inversion strategy is the double-difference time-lapse waveform inversion (DDWI) (inversion of the difference data starting from the reverted baseline model). It is an effective way to solve the problem of that baseline and monitor inversions of time-lapse waveform inversion are easy at different convergences resulting in coherent model error in time-lapse inversion. Nevertheless, DDWI demands a mostly perfect repeatability between baseline and monitor surveys, which is the most tough challenge for it. Specially, when source wavelets for baseline and monitor data sets are different, the results of DDWI are impacted seriously. To solve this problem, we propose a double-wavelet double-difference time-lapse waveform inversion mothed (DWDDWI). It works because the data difference caused by the wavelet difference is eliminated. DWDDWI is developed based on the convolution relationship between the shot gather and Green's function. And its premise is that the wavelets for both baseline and monitor data sets are known. To test the feasibility of this mothed, a numerical example is used.

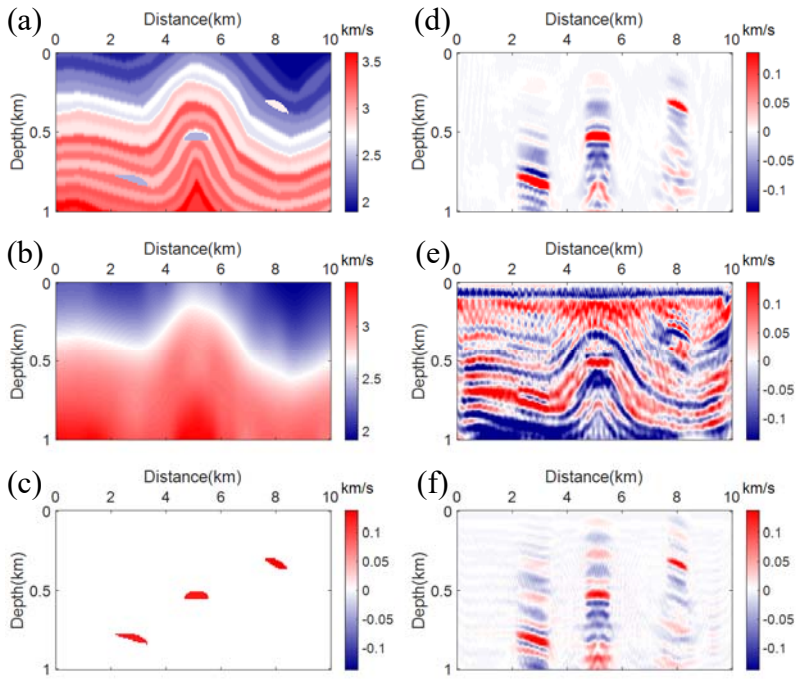

FIG. 1. (a) The true baseline model, (b) the initial baseline model, (c) the true monitor model. (d) The inverted monitor model by DDWI when the wavelets for baseline and monitor data are the same. (e) The inverted monitor model by DDWI when the wavelets for baseline and monitor data are different. (e) The inverted monitor model by DWDDWI when the wavelets for baseline and monitor data are different.

Waveform inversion combining one-way and two-way wave-equation migration

Xin Fu, Sergio Romahn, and Kris Innanen

ABSTRACT

Growing out from FWI, iterative modelling, migration, and inversion (IMMI) considers waveform inversion as a cyclical process of the migration and standard inversion. In IMMI, any type of depth migration is available, which gives greater convenience to waveform inversion. Much research has shown that IMMI with the control of well log data is an effective method for waveform inversion. However, how to perform IMMI in the absence of well log data has not systematically investigated. In this paper, we examine IMMI in the absence of well log data. we introduce how to choose impedance inversion algorithms in IMMI for different depth migration algorithms. And we suggest employing the trace integration algorithm in frequency domain for a one-way depth migration based on the one-way wave equation, and the impedance inversion algorithm without phase change for a two-way depth migration based on the two-way wave equation. In our research, the one-way depth migration algorithm used is phase shift plus interpolation (PSPI) migration, and the two-way depth migration algorithm used is reverse time migration (RTM). Built on this, we develop a combined IMMI method which uses the one-way depth migration and the two-way depth migration sequentially in IMMI. To do comparisons between FWI, IMMI using PSPI migration, IMMI using RTM, and the combined IMMI method, two numerical examples are used. The comparisons show that IMMI using RTM and using PSPI are better than FWI, and the best wave to implement waveform inversion in the absence of well log data is the combined IMMI method.

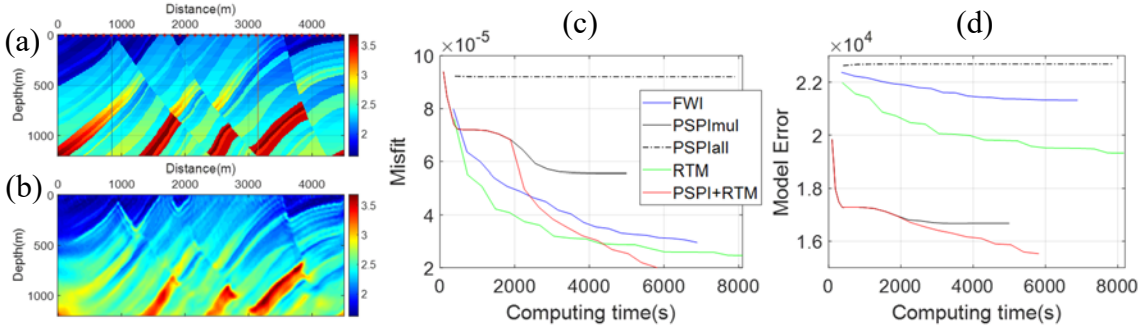

FIG. 1. (a) The true P-wave velocity model, (b) the inverted model. (c) Data misfit versus computing time, (d) model error versus computing time, and the red curves correspond to the combined IMMI method.

Machine learning as a tool to predict oil saturation from well logs

Marcelo Guarido* and Daniel Trad

ABSTRACT

Oil saturation is the measure of the amount of oil inside the porosity of a reservoir rock. Its calculation, usually from core analysis, is an important quantity that helps to characterize the reservoir. In this work, we are not predicting the actual oil saturation due to the lack of information for the wells gathered, but the fraction of mass of oil in the core. Most of this report is focused on the data preparation prior to modeling, as our variables and targets came from two different measurement sources (well logs and core analysis), and in how to create a valid workflow to make features and targets compatible to each other. In the end, we show how to select an appropriate machine learning model to predict the target, which need to be one with non-linear properties, and how to interpret the feature importance. To predict the fraction of mass of oil, the induction log ILD is the one that brings most of the information, but it needs to be combined with other logs for the prediction to make sense. The metric used to evaluate the models was the R^2, and the best model had a score of 0.82.

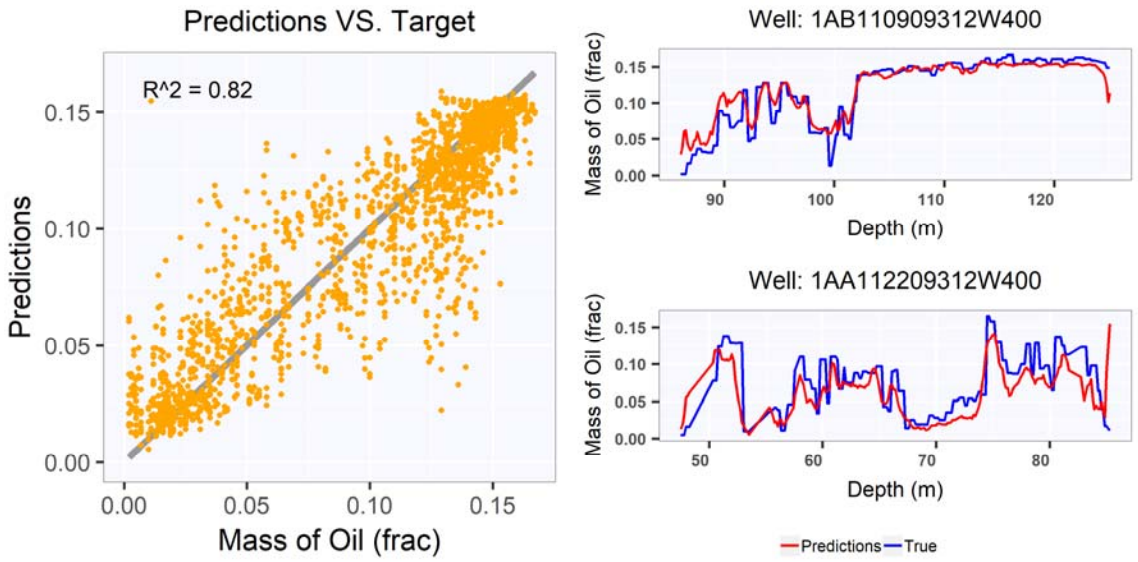

FIG. 1. Predictions using a gradient boosting regressor. On the left is shown the cross plot between true data and predictions, with a R^2 of 0.82. On the right are two examples of true mass of oil (in blue) and predictions (in red) in specific wells.

Using natural language processing and machine learning to predict severe injuries classification in the oil and gas industry

Marcelo Guarido and Daniel Trad

ABSTRACT

Severe injuries, such as fractured body parts and amputations, are always on the top list of mitigation importance in any job. In this work, we use the incident/accident description of the severe injuries' reports from the Occupational Safety and Health Administration of the United States Department of Labor to create a machine learning model that standardizes the class of the incident classification. We used natural language processing to convert each description of an injury to numerical features and applied the TF-IDF methodology to remove words that are not important on the classification of an injury. Models such as "Extremely Randomize Trees" and "Multinomial Logistic Regression" were trained and applied on the oil & gas industry's reports to test their accuracy, and we came to the following conclusions: predictions are improved when binary input features are used; the Extremely Randomized Trees tends to predict the most frequent classes with accuracy over 80%; the Logistic Regression works better for the other classes with balanced accuracy of 54% if implemented with balanced class weights.

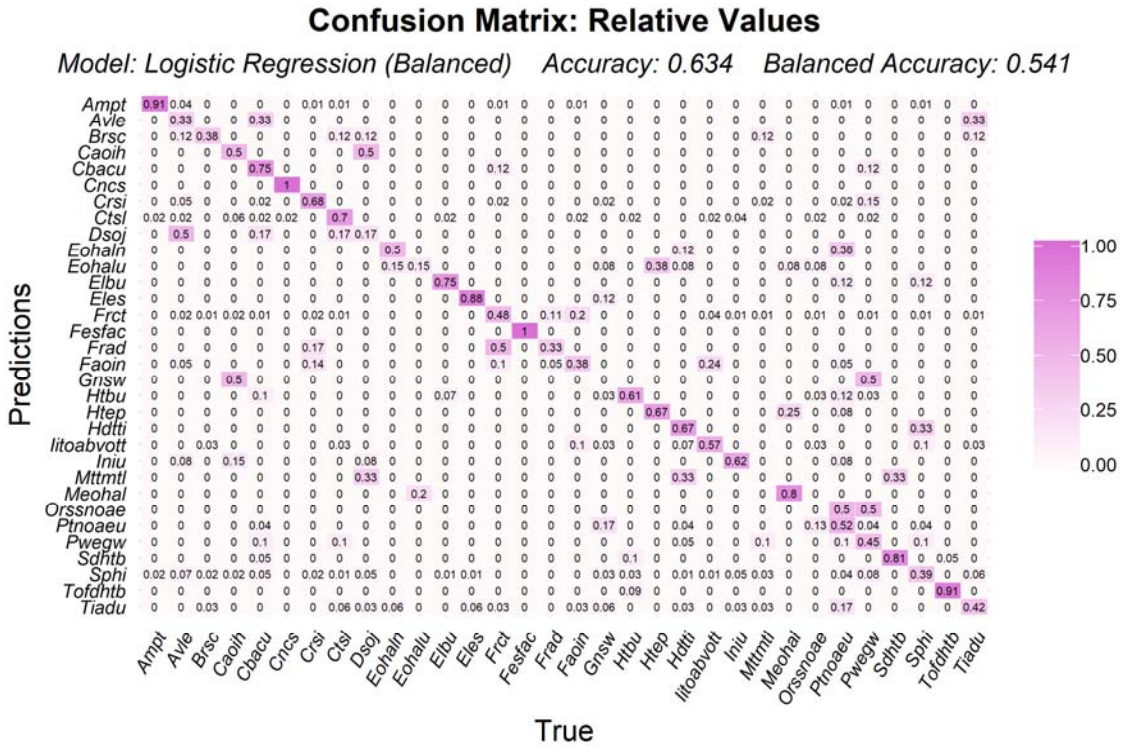

FIG. 1. Confusion matrix for the logistic regression model with balanced class weights and binary features.

SS-wave reflections from conventional 3C data

Saul E. Guevara and Daniel Trad

ABSTRACT

This is an experiment with real data intended to identify the presence of pure S wave reflections (SS-waves) generated by conventional explosive sources. Just PP and PS waves are usually expected on these surveys. The horizontal components of the Hussar 2011 3C survey were used to this purpose. From the velocity information, the SS-wave would arrive inside the Ground Roll cone. Therefore noise attenuation for events such as surface waves, simultaneously preserving as much as possible the expected SS-waves. The resulting records show feasible SS-events, energy with the expected arrival time in both radial and transversal components, however appear easier to identify in the transversal component. An experiment for S-wave source static corrections allowed to obtain an SS stack section, which is illustrated by the Figure, compared to a PS stack section. Some events can be identified at the expected arrival time. The method appears promising to obtain additional information of 3C data.

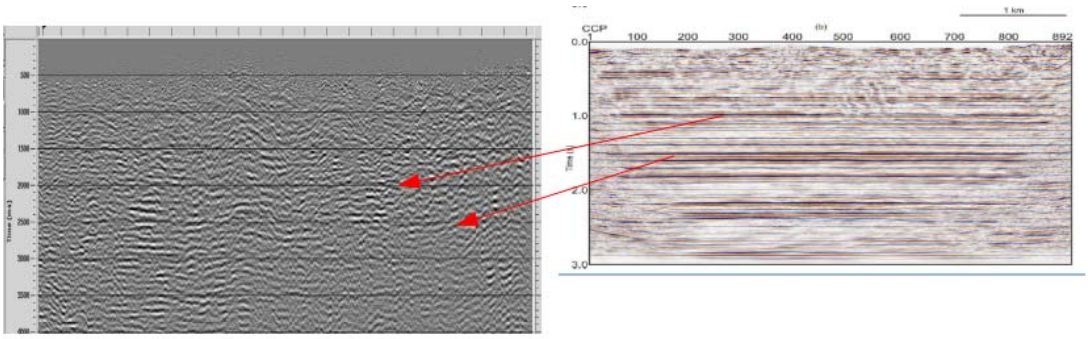

FIG. 1. Stacked section of the transversal component (left-hand side) after source statics correction and applying an SS velocity model. As for comparison, the PS-wave section of the same seismic line (right-hand-side), and the corresponding arrival of events shown by arrows.

DAS trace location assignment for the CaMI.FRS fibre loop

Kevin W. Hall and Don C. Lawton

ABSTRACT

As our knowledge of the optical fibre loop at the Containment and Monitoring Institutes Field Research Station (CaMI.FRS) continues to evolve, we are able to assign *x*,*y* and *z* coordinates to seismic traces recorded upon the loop using various DAS interrogators. For example, gyroscopic surveys conducted on observation wells 1 and 2 (OBS1 and OBS2) in the past year show that neither well is perfectly vertical. Using this updated information, we have built a trace geometry model that can be easily adjusted for varying trace spacings, uncertain cable lengths, fibre indices of refraction (actual and as used in interrogator software), and other unknowns. For downhole data with up- and down-going fibre, we may exploit symmetry by coarsely locating the bottom of the well using cross-correlation, fine-tuning using stack-power in sliding windows over a small trace range (+/- 5 traces), and applying the geometry from our model. This strategy works well even for noisy shots, where cross-correlation by itself gives slightly varying answers from shot to shot. Quality control of observation well data thus far has been by inspection of interleaved up- and down-going DAS data sorted by true vertical depth (Figure 1) as well as stacks and residuals. Comparisons of straight and helical fibre data from the wells and the trench have not progressed beyond interleaving data sorted by true vertical depth or easting. Stacking straight and helical data will require a careful trace interpolation step to compensate for differing effective trace spacings.

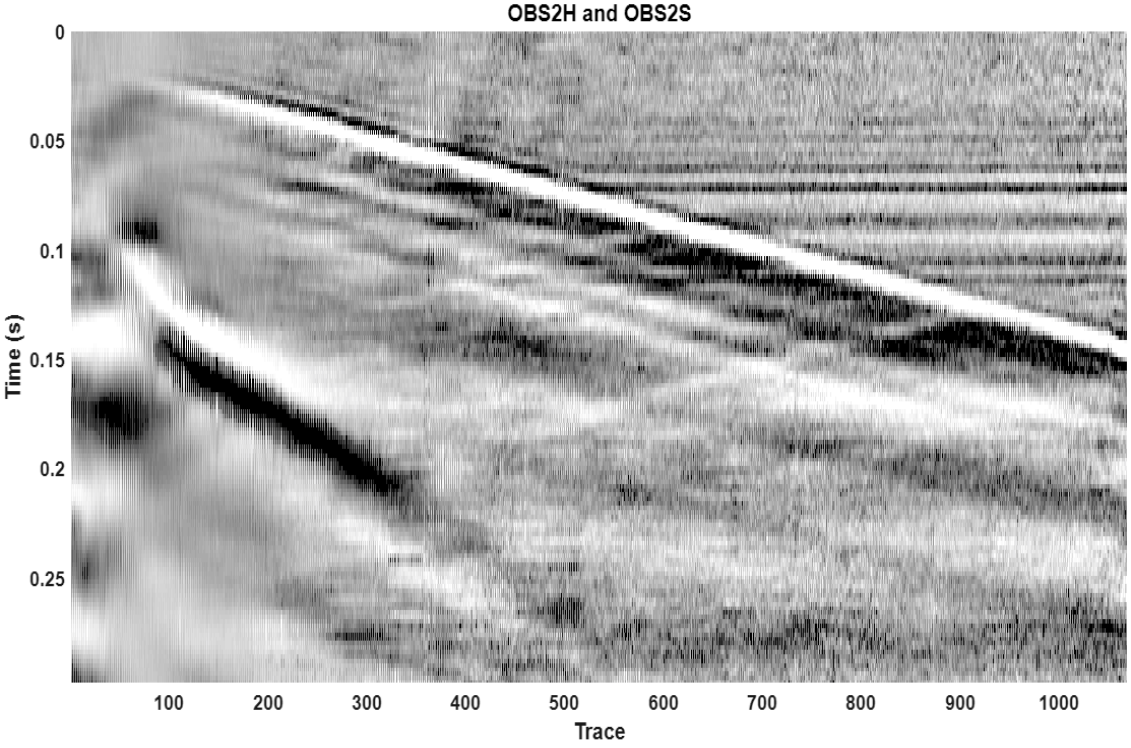

FIG. 1. Straight and helical fibre data in the OBS2 well sorted by TVD after loading geometry into trace headers.

A directional DAS sensor and multi-component geophone comparison

Kevin W. Hall* and Kris Innanen

ABSTRACT

Two surveys were acquired at the Containment and Monitoring Institute Field Research Station (CaMI.FRS) in 2018 that have common shots recorded on optical fibre (strain-rate; VSP and directional DAS surveys), geophones (velocity; VSP and directional DAS surveys), and accelerometers (acceleration; VSP survey only). Accelerometer data may be integrated to compare to geophone data, and we propose to further convert integrated accelerometer and unmodified geophone data to strain-rate by simply subtracting two traces, dividing by the distance between them, and plotting the result at a position halfway between the original traces (Figures 1 and 2).

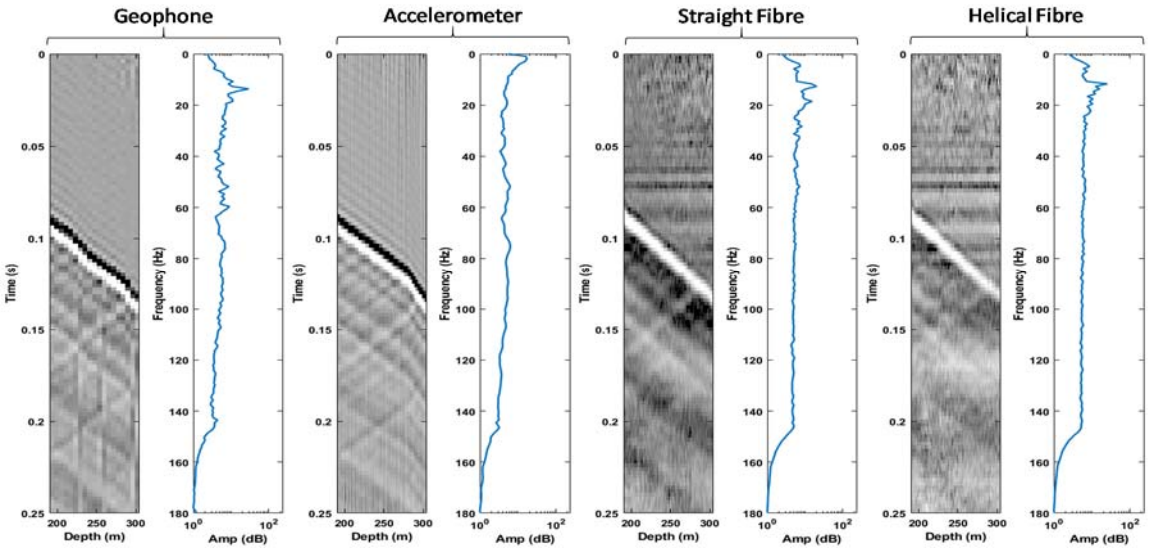

FIG. 1. VSP showing vertical component geophone (left) and accelerometer data (center left) converted to strain-rate for comparison to straight (center right) and helical (right) fibre data.

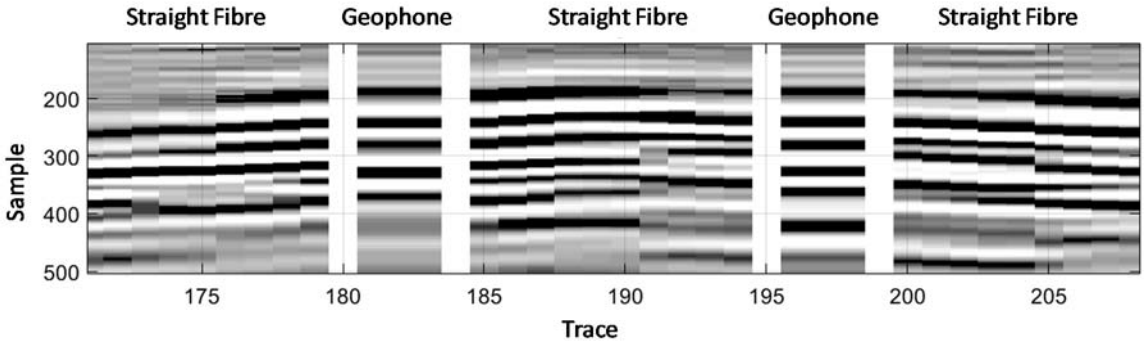

FIG. 2. Straight fibre data from directional DAS survey compared to horizontal component geophone data that have been rotated to be inline with a given fibre segment and then converted to strain-rate.

Comparison of straight and helically wound fibre-optic cables in distributed acoustic sensors

Heather K. Hardeman-Vooys and Michael P. Lamoureux

ABSTRACT

In this paper, we provide insight into the amplitude response of a distributed acoustic sensor. Using techniques from algebraic topology, we know that there is a mathematical foundation for deforming a helically wound fibre into a straight fibre for a DAS system. We model what occurs as a helically wound fibre deforms into a straight fibre optic cable. The deformation allows us to consider how the strain tensor is affected by studying its determinant, trace, and eigenvalues.

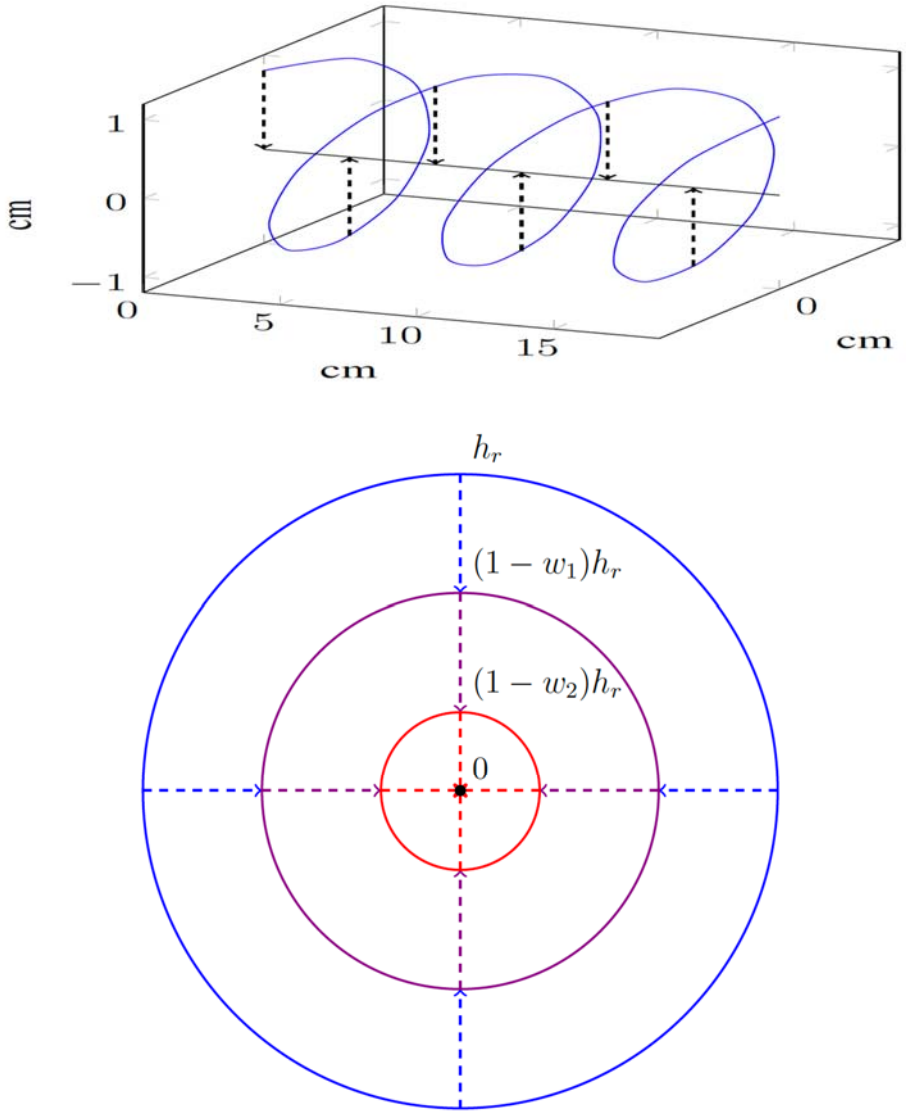

FIG. 1. (Top) A helix of radius 1 inch deforming into a straight line. (Bottom) A 2π cross-section of a fibre-optic cable with helical radius h_r deforming into a straight fibre over four choices of w.

Event detection using independent component analysis and Gaussian mixture models

Heather K. Hardeman-Vooys*, Matt McDonald, and Michael P. Lamoureux

ABSTRACT

Inspired by the work of Shamsa and Paydayesh (2019) who used Gaussian mixture models and independent component analysis to analyze microseismic data, we apply the methodology to data collected using a distributed acoustic sensor in order to detect a vehicle driving along a DAS system. We introduce Gaussian mixture models and independent component analysis. Then, we provide two examples where we calculate two independent components, the vehicle's signal and the noise, before training a Gaussian mixture model to detect the signal. We consider two methods of training the Gaussian mixture model and compare the results.

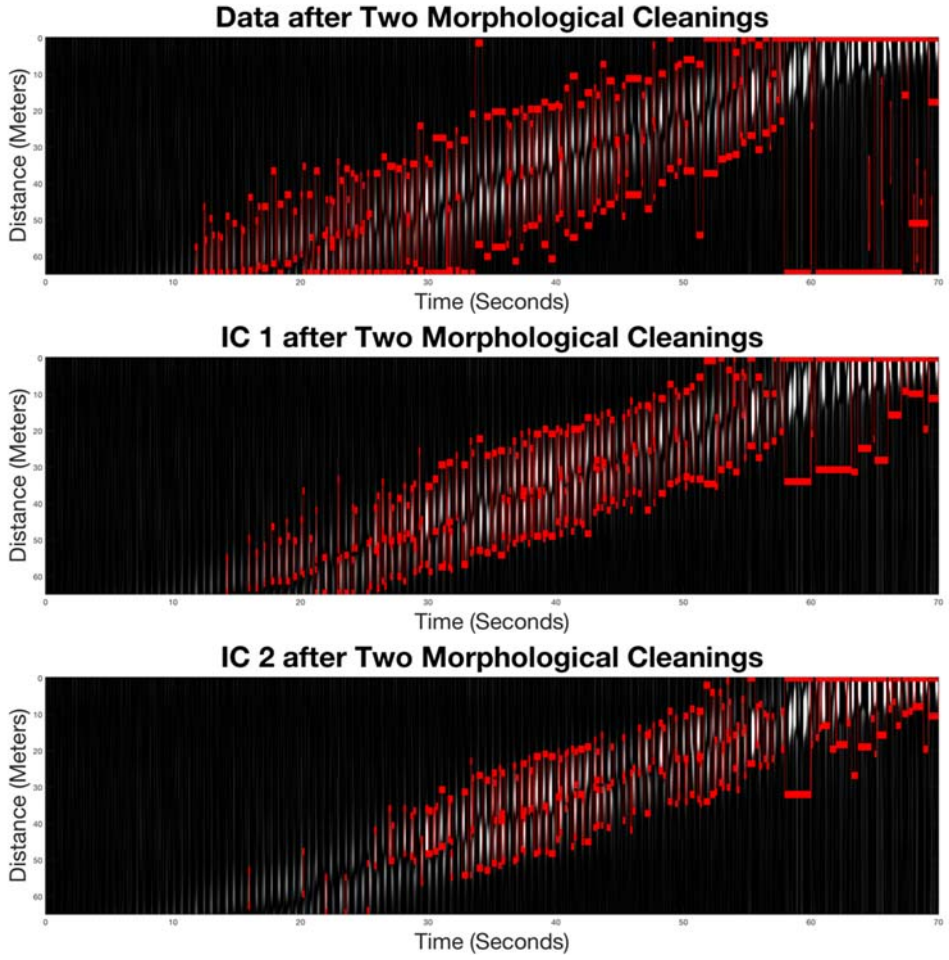

FIG. 1. (Top) The results of the vehicle detector trained on the training data applied to the test data after two morphological cleanings. (Middle) The results of the vehicle detector trained on a window moving over the first independent component applied to the test data after two morphological cleanings. (Bottom) The results of the vehicle detector trained on a window moving over the second independent component applied to the test data after two morphological cleanings.

Image registration for distributed acoustic sensing acquired data using convolutional neural networks

Heather K. Hardeman-Vooys, Matt McDonald, and Michael P. Lamoureux

ABSTRACT

We provide a brief overview of convolutional neural networks. Then we introduce a training set extracted from real data. We test the trained convolutional neural network on a portion of the training set to determine accuracy. Afterwards, we employ this trained convolutional neural network to identify events in data which contains walking and digging events. We then discuss our results which suggests that more than just the source of an event affects the way the event looks in the data.

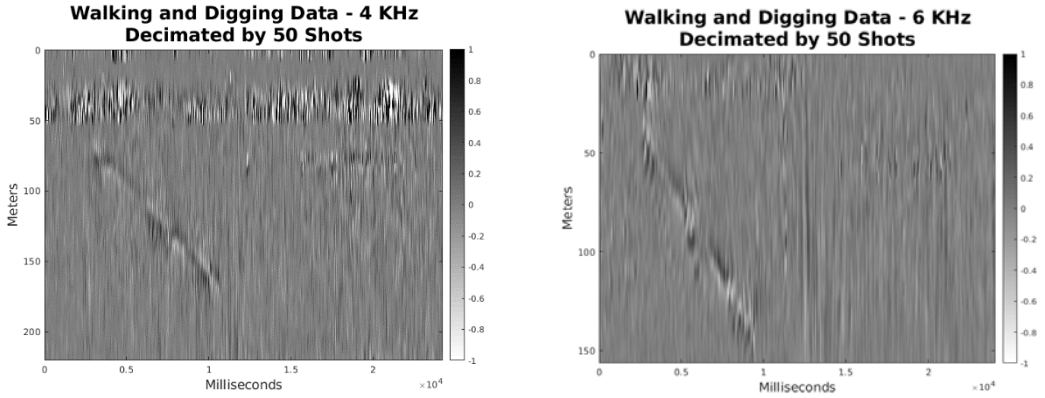

FIG. 1. Two samples of DAS data showing walking and digging, at different recording frequencies. On the left image, the diagonal feature from 50 to 200 meters is someone walking while the horizontal feature are 50 meters is someone digging. On the right graph, the diagonal feature from 25 to 150 meters is someone walking, while the horizontal feature at 25 meters is digging.

	Test Set	No Decimation	10 Shots	50 Shots
Test	80%			
4kHz		11%	34%	77%
6kHz		9%	0%	39%

TABLE. 1. The accuracy of the convolutional neural network for identifying events correctly in each type of 4kHz PRF and 6kHz PRF acquired walking and digging data.

Let there be light: illuminating physical models from the surface

David C. Henley* and Joe Wong

ABSTRACT

A complex physical model should be illuminated by seismic energy over as wide an observation aperture as possible, in order to adequately image all the details of the model. Ideally, this aperture would consist of 360deg of uniform raypath coverage of the model features, and the resulting images should then accurately capture the model details for interpretation. Realistically, in a field setting, however, we can rarely illuminate a target over more than a small fraction of the ideal aperture. Hence, we explore here how well we can detect and characterize the features of a target using reflection data acquired over a restricted aperture; for example, data recorded on the accessible upper surface of the model, representing 90deg or less of aperture.

A complex physical model was constructed at the CREWES physical modeling facility to explore illumination by various combinations of sources and receivers, including subsurface positions utilizing both vertical and horizontal boreholes. Several complete seismic model surveys were conducted using this model. From the available survey data sets, we selected a multi-fold conventional 2D survey and a high-spatial-resolution single-fold zero-offset survey to investigate how much detail we could observe or deduce about the physical model, using only sources and receivers located on the upper surface of the model.

Strong coherent noise (mostly reflections from the modeling tank) appears in both data sets, and we demonstrated techniques for attenuating the noise on both data sets. We then formed various images from each data set and analyzed the model features seen on each image. Surprisingly, the single-fold high-resolution image reveals more interpretable model detail than the multi-fold CMP stack image. The figure below shows this data set with a schematic of the model superimposed.

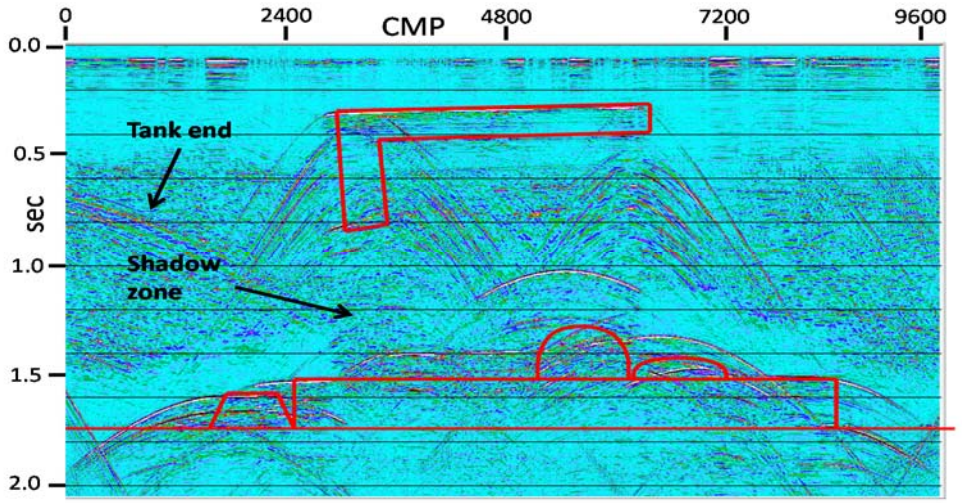

Direct elastic FWI updating of rock physics properties

Qi Hu*, Scott Keating, and Kris Innanen

ABSTRACT

Quantitative estimation of rock physics properties is of significant interest in reservoir characterization, and most current workflows with this subject are based on amplitude variation with offset (AVO) techniques. With the expectation of more accurate results, we propose to directly estimate rock physics properties using elastic full-waveform inversion (FWI). We implement this by incorporating the rock physics model, which builds a link between elastic and rock physics properties, into the FWI workflow to reformulate the model parameterization using rock physics parameter classes. We consider three rock physics models: the Han empirical model, the Voigt-Reuss-Hill (VRH) boundary model, and the Kuster and Toksöz (KT) inclusion model. Each is used to formulate a model parameterization of porosity, clay content, and water saturation (P-C-S). We employ the truncated-Newton optimization method to update the model by iteratively minimizing the differences between synthetic and observed data. With numerical examples, our method shows considerable promise for recovering rock physics properties. It also possesses advantages over a sequential approach, which first invert for elastic attributes, then recover rock physics properties from them. We note that the Han model gives the most accurate results, whereas the KT model recovers the models with the largest errors. These large errors likely originate from the higher degree of nonlinearity of the KT model. The analytical radiation patterns of the P-C-S parameterization illustrate that the perturbation of water saturation has a minor effect on seismic data, this explains why water saturation is more challenging to recover compared with the porosity and clay content in our examples.

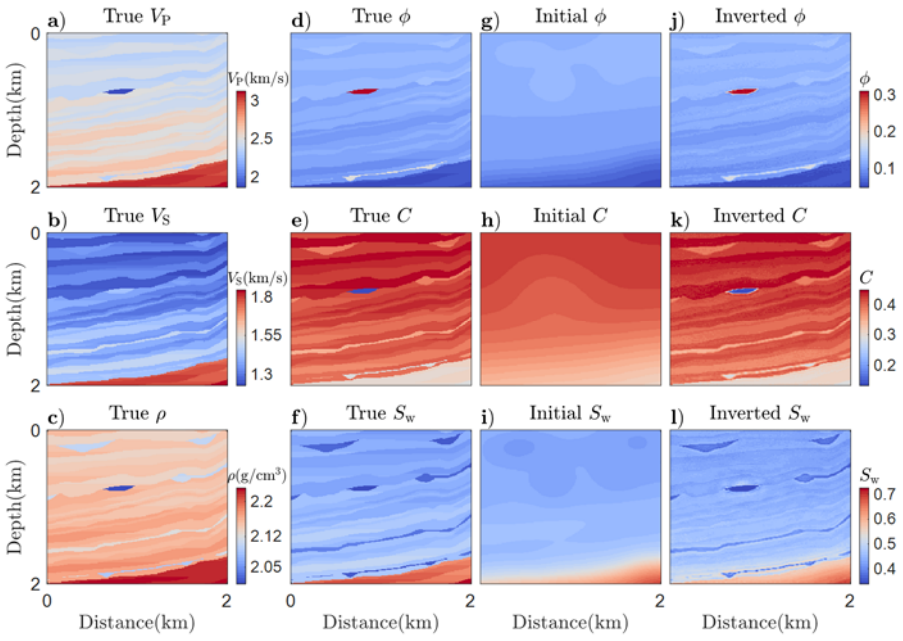

FIG. 1. (a-c) True models of P- and S-wave velocities, and density. (d-f) True models, (g-i) initial models, and (j-l) the corresponding inversion results of porosity, clay content, and water saturation.

Study of crosstalk reduction in multiparameter acoustic FWI

Qi Hu and Kris Innanen

ABSTRACT

Crosstalk is the phenomenon in which data signatures of different physical properties are confused in full-waveform inversion (FWI). The challenges associated with crosstalk are a major obstacle to the effective implementation of multiparameter FWI. In this study, we focus on acoustic media with variable density, and discuss about the reduction of parameter crosstalk from three aspects: optimization method, acquisition geometry, and model parameterization. Optimization methods such as steepest-descent, conjugate gradient, and quasi-Newton methods are compared in terms of inversion quality and computational cost. For geometry, we show how sub-surface sources and receivers provided by vertical seismic profile (VSP) and crosswell can help mitigate the crosstalk from surface seismic. Scattering patterns of four parameterizations: velocity-density, impedance-density, impedance-velocity, and bulk modulus-velocity, are illustrated and employed to study their capabilities relative to crosstalk.

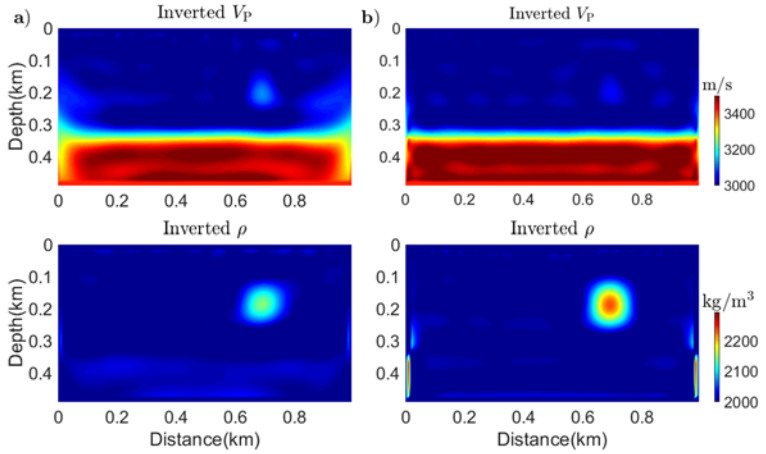

FIG. 1. Comparison of the inverted velocity V_P, and density ρ using a) surface seismic, and b) VSP + surface seismic.

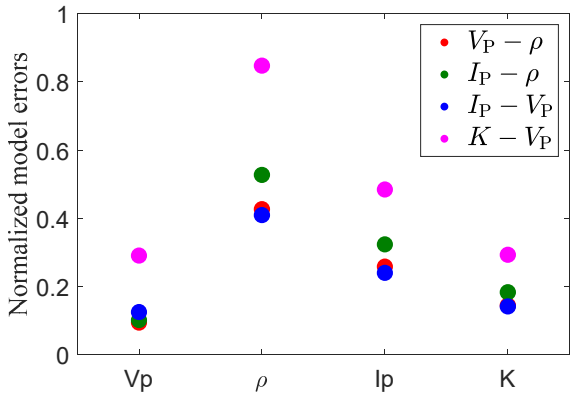

FIG. 2. Normalized model errors of inverted velocity V_P, density ρ, impedance I_P, and bulk modulus K with different parameterizations.

Migration with surface and internal multiples

Shang Huang* and Daniel Trad

ABSTRACT

Multiples can provide additional information for subsurface structures compared with primary reflections. In this paper, we consider two different uses of multiples for imaging. First, we will look at the use of the first-order surface multiples for reverse time migration (RTM). Observed primaries are extracted from shot records and injected as virtual sources and surface multiples are used as data and back-propagated in time. Then the cross-correlation between primary wave and the first-order surface multiple is used as image condition. RTM of surface multiples gives a more extensive illumination than RTM of primaries. In addition, least-squares reverse time migration (LSRTM) of surface multiples presents improved vertical resolution compared with RTM. Also, LSRTM of the first-order surface multiple can recover the information from upper-side dipping events as well as some small flanks. The main requirement of these benefits is, however, quite challenging: to achieve multiple separation before migration.

The second use of multiples we examine here is full-wavefield migration (FWM). This method uses an inversion-based approach to update the subsurface image. Reflection coefficient updates are obtained from scattering effects, including reflections and differential transmissions. A horizontal-layered model is used for proving the benefits of using FWM. Forward modeling by phase shift plus interpolation derives stable downgoing and upgoing wavefields separately, which can predict primary, surface multiples and internal multiples in a full-wavefield response. FWM of total wavefields can provide more details in the image compared with FWM of primary only. Adding energy from multiples into migration is not a replacement for migrating primary reflections, but it can be a useful complement to improve the image resolution and illumination for an accurate geological interpretation.

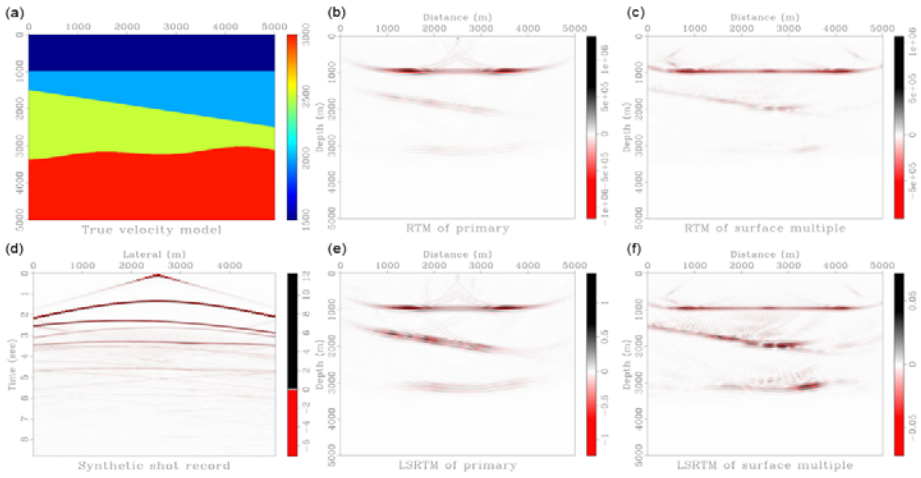

FIG. 1. Example for testing the image quality of RTM and LSRTM with the first-order surface multiple. (a) True velocity model. (b) RTM of primary wave. (c) RTM of the first-order surface multiple. (d) Synthetic shot record where the shot was at the central horizontal distance. (e) LSRTM of primary wave after 5 iterations. (f) LSRTM of the first-order surface multiple after 5 iterations.

Deblending using hybrid Radon transform

Amr Ibrahim, Kai Zhuang, and Daniel Trad

ABSTRACT

In this report, we add a hybrid Radon transform to the inversion-based deblending method. Deblending methods that use sparsity constraint relies on the similarity between the primary signal and the transform basis. This similarity results in the focusing of the coherent primary signal while simultaneously attenuating the incoherent blending noise. However, seismic data contains mixtures of signals with different travel time trajectories. Therefore, using hyperbolic functions to model seismic data that contains non-hyperbolic events will reduce sparsity (signal focusing) and thereby reduce the efficiency of the deblending algorithm. To overcome this issue, we expand the transform basis to account for more types of signals contained in the seismic data. In this report, we a hybrid of linear and hyperbolic Radon basis functions to match the moveout patterns of reflections and direct arrivals. Synthetic data examples show that this transform can efficiently deblend seismic reflections and direct arrivals, as shown in the following figure.

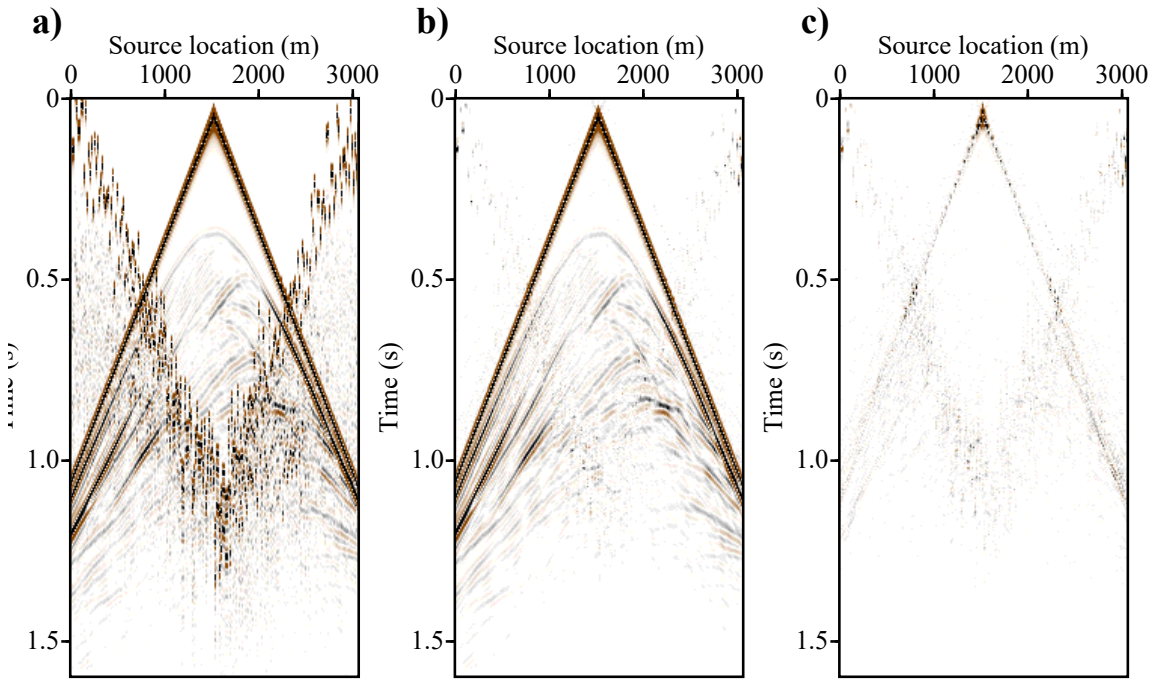

FIG. 1. Marmousi model synthetic data example. (a) Common receiver gather (CRG) with blending noise. (b) Inversion-based deblended CRG. (c) Deblending error.

Deblending using robust inversion of Stolt-based Radon operators

Amr Ibrahim* and Daniel Trad

ABSTRACT

In this report, we compare the denoising and inversion-based methods for deblending using Stolt-based Radon operators. These operators are used to construct a robust inversion problem with a sparsity constraint. Sparsity promoting transforms, such as Radon transform, can focus seismic data and produce a sparse model which can be used to separate signals, remove noise, or interpolate missing traces. For this reason, Radon transforms are a suitable tool for deblending. We can incorporate Radon transform into the deblending problem in two ways, either using denoising based or an inversion-based approach. The denoising based method treat blending interferences as random noise by sorting the data into new gathers, such as common receiver gathers. In these gathers, blending interferences exhibit random structures due to the randomization of the source firing times. On the other hand, the inversion-based method treats blending interferences as a signal, and the transformation can model this signal in the Radon domain by incorporating the blending operator to formulate an inversion problem. We compare both methods using sparse inversion in the hyperbolic Radon domain. Synthetic and field data examples show that the inversion-based approach can produce more accurate separation and better convergence. However, the inversion-based method increases the computational cost of deblending.

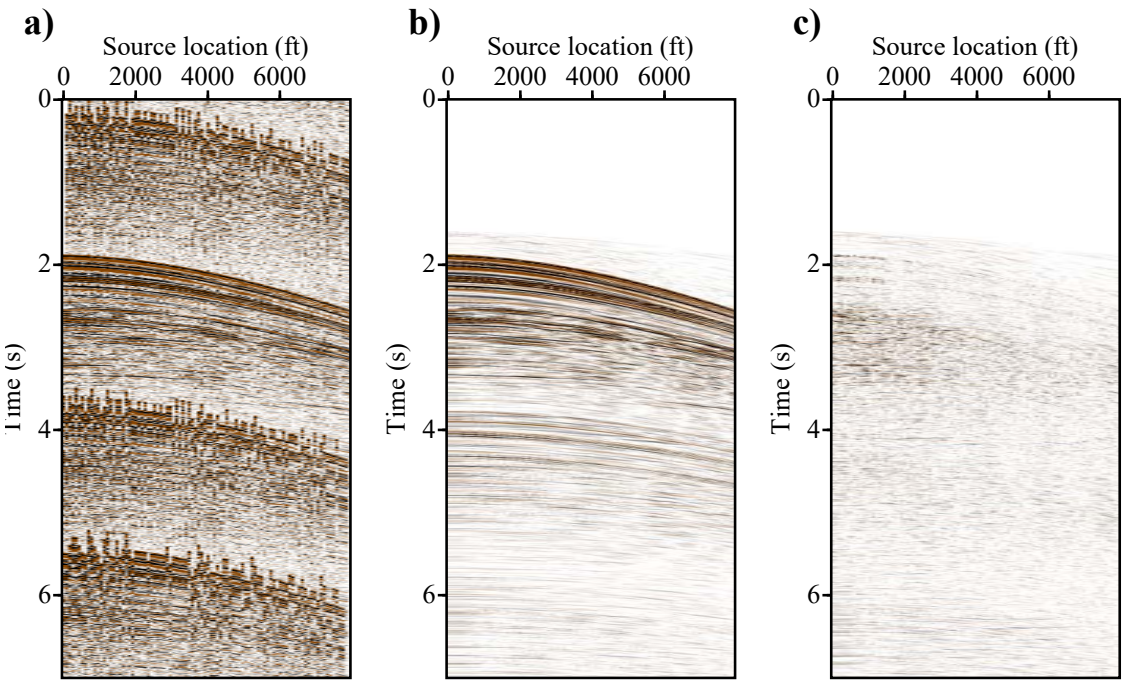

FIG. 1. Gulf of Mexico data example. (a) Common receiver gather (CRG) with blending noise. (b) Inversion-based deblended CRG. (c) Deblending error.

Detection of transient time lapse seismic signatures associated with CO_2 injection

Kris Innanen*, Don C. Lawton, Kevin W. Hall, Kevin L. Bertram, and Malcolm Bertram

ABSTRACT

In 2018 CREWES researchers reported on a collaboration with JOGMEC researchers in interpreting an unusual time-lapse data set, in which cross-well waveforms transiting a region in which microbubble water had been injected were seen to undergo several difficult-to-explain alterations. In addition to attempting to explain these phenomena, we also undertook to seek similar variations in seismic waveforms propagated through the plumes of CO2 being injected into the 300m formation at the CaMI-FRS in Newell County AB. Here we report on the experiment and set out some of our early observations. We establish remarkably repeatability with the Envirovib source placed pad-down throughout the 160hr experiment. On this backdrop, which was favourable for time-lapse analysis, we identify several spectral variations, some of which appear and then vanish over the course of the experiment; of these many of the changes exceed several standard deviations as estimated during repeatability tests, and thus do appear to be "real" variations connected to the injection. The changes are in general not inconsistent with our 2018 "elastic bracing" explanation, but they appear to be much more complicated and quite subtle, and we stop short of offering a mechanism for what we see while analysis continues.

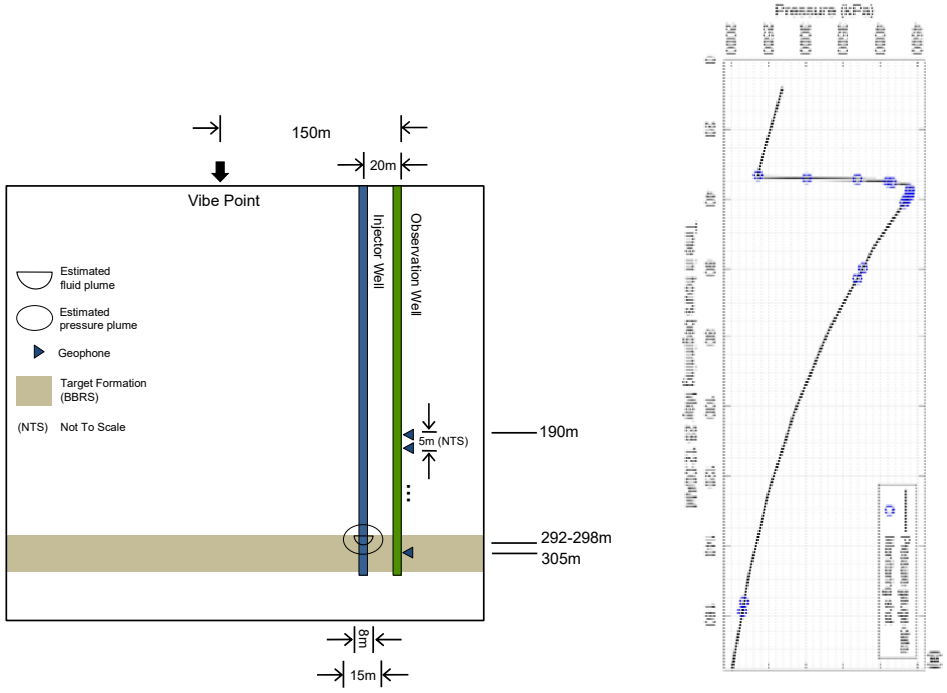

FIG. 1. Left panel: schematic diagram of injection and monitoring experiment, including source location, geophone depths, injection well and estimated size of injection plumes (pressure and fluid). Right panel: time line of injection pressure (solid) with the times of the monitoring shot clusters overlain in blue.

Quantitative characterization and monitoring of reservoir properties, pressures, fluids and fractures with multicomponent and quasi-continuous full-waveform seismology

Kris Innanen, Daniel Trad, Don C. Lawton, Rachel Lauer, Roman Shor, and Michael Lamoureux

ABSTRACT

Full waveform (FWI) seismic methods have achieved spectacular industrial and academic successes in image-forming of complex offshore reservoirs, but as practical, regular-use tools for monitoring of onshore conventional and unconventional production, CO_2 and wastewater injection, and EOR methods, basic and applied scientific progress is still required. Fortunately, geophysicists now have at hand powerful new geo-computational tools, HPC and artificial intelligence technology, and new instrumentation and seismic acquisition tools, in the form of permanent controllable sources, broadband geophones and distributed acoustic sensing (DAS, or fibre-optic) seismic sensors, and drillstring acoustic technology. We propose to create the next generation of practical, FWI reservoir characterization and monitoring tools, involving the determination of high resolution maps of rock physics properties – pressures, fluids, fractures and viscosities – through analysis of the elasticity, viscosity, and anisotropy of the complex modern reservoir environment. Our group has carried out significant, though initial, research in broadband and fibre-optic field and laboratory acquisition, practical multi-parameter elastic, viscoelastic and anisotropic FWI method development, rock-physics seismic inversion, near surface characterization, drillstring imaging, machine learning, and HPC methods for large computation/data problems. We propose to grow and expand these early successes, creating a practical reservoir waveform package. FWI involving multicomponent and DAS data, elastic FWI-rock physics sensitivity analysis, surface wave analysis and processing, machine learning for seismic inversion, and new blended acquisition / deblending methodologies, are key outcomes of the research.

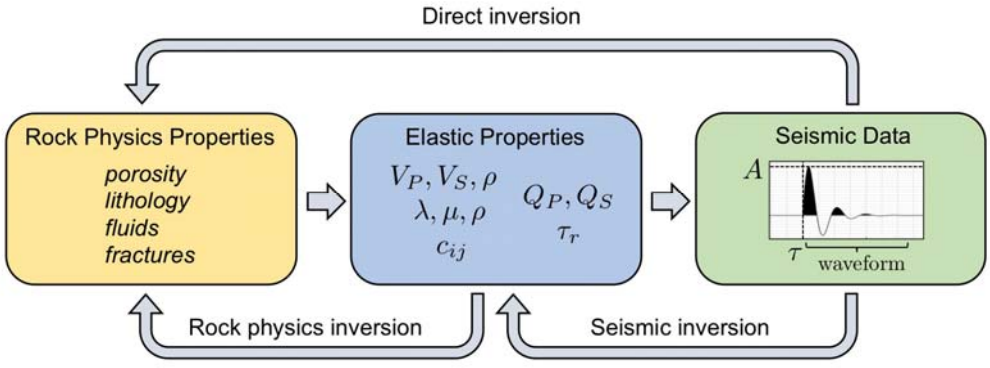

FIG. 1. A well-known pair of approaches to rock physics inversion with seismic amplitudes. Setting out practical, field-validated formulations of both of these routes with elastic full waveform methods is the core aim of the CREWES proposal.

Short note: analysis of the non-uniqueness of seismic travel-times through brute-force counting

Kris Innanen

ABSTRACT

How hard seismic inversion is, and how good a solution we can expect, both rest on the uniqueness of a seismic datum (such as a travel time), and then the degree to which multiple independent data of the same type can mitigate it. Since large numbers of unknowns are involved, one might think to use the methods of statistical mechanics to characterize this non-uniqueness. Such analyses usually start with a counting of possibilities (e.g., the number of states of a many-particle system with the same energy). In our case the counting would be of the number of the possible models which produce the same traveltime (or amplitude, or waveform component, etc.). How precisely can we count the number of discrete slowness models which produce a given traveltime? Here we will set out an approach in a short note. Once we have a method for counting, we may be able to glean interesting facts about the inverse problem in a range of experiments and seismic source/receiver configurations.

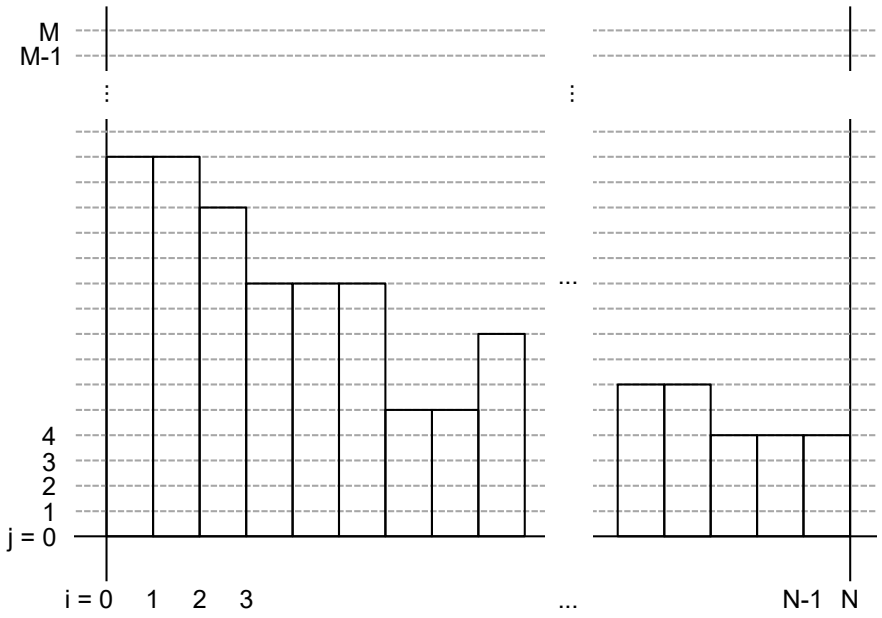

FIG. 1. A discretization of the slownesses along a ray path length. The non-uniqueness of the inverse problem is somehow quantified by the fraction of the total number of possible models of this type which produce the same traveltime.

Seismic studies of the near-surface at the CaMI Field Research Station in Newell County, Alberta

J. Helen Isaac and Don C. Lawton

ABSTRACT

We reassessed the processing and analysis of the two S-wave seismic surveys that were acquired at the CaMI Field Research Station (FRS) in the summer of 2018. We refined the S-wave depth/velocity model derived from refraction statics analysis of the S-wave fixed array data by limiting the offsets in the analysis. The new model shows a 19-26 m thick near-surface layer with velocities ranging from 222 to 288 m/s. Below this layer is bedrock with S-wave velocities between 885 and 930 m/s. The depths to bedrock compare well with the actual bedrock depth at the injection well location. The profile of the near-surface S-wave velocity corresponds well with the refractor depth profiles obtained through refraction analysis of 2D P-wave data (Figure 1).

We also improved the imaging of the S-wave streamer data by reprocessing the data. We rebinned the CDPs and applied updated stacking velocities. We also applied pre-stack trace mixing and post-stack f-x deconvolution because of the very short receiver spacing of 1 m and low fold. The resulting reflector is more continuous and better focussed. However, we found that the observed time structure is highly sensitive to changes in the stacking velocities, as they are so low.

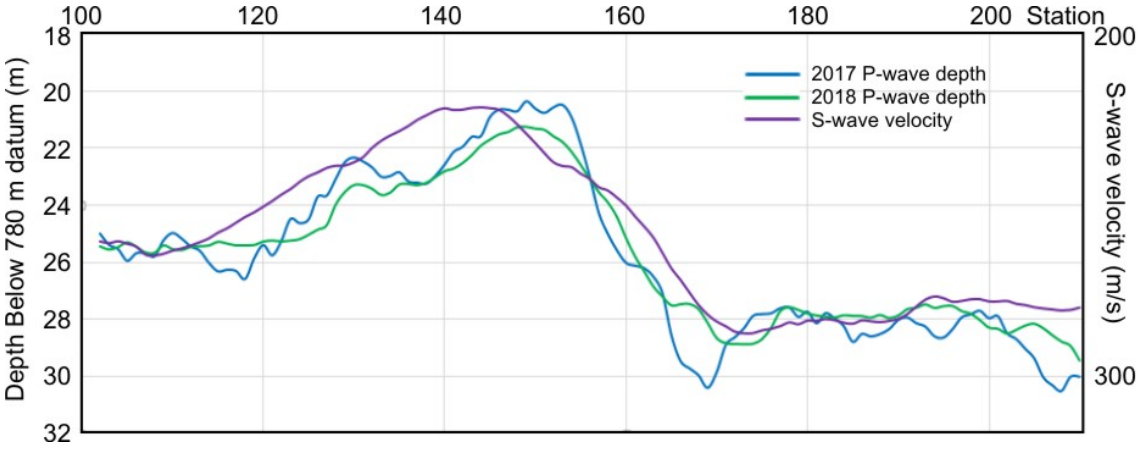

FIG. 1. The refractor depth models derived from analysis of the 2017 2D P-wave surveys with the S-wave near-surface velocity overlain.

Accounting for attenuation in the downward generator adaptive subtraction domain

Scott Keating*, Andrew Iverson, and Kris Innanen

ABSTRACT

Inverse-scattering based internal multiple prediction strategies suffer from inaccuracies in the predicted amplitudes. A notable source of these discrepancies is mistreatment of transmission losses by the conventional prediction algorithm. Interface-related transmission losses have been previously discussed, but artifacts from wave attenuation impair the predictions in much the same way, and potentially to a larger extent. Compensating for these errors with a conventional adaptive subtraction is problematic: the attenuation-related errors do not vary consistently as a function of the prediction dimensions. Here, we illustrate that attenuation errors are highly predictable in downward-generator space, and that adaptive subtraction in the downward-generator-prediction space is capable of compensating for attenuation errors.

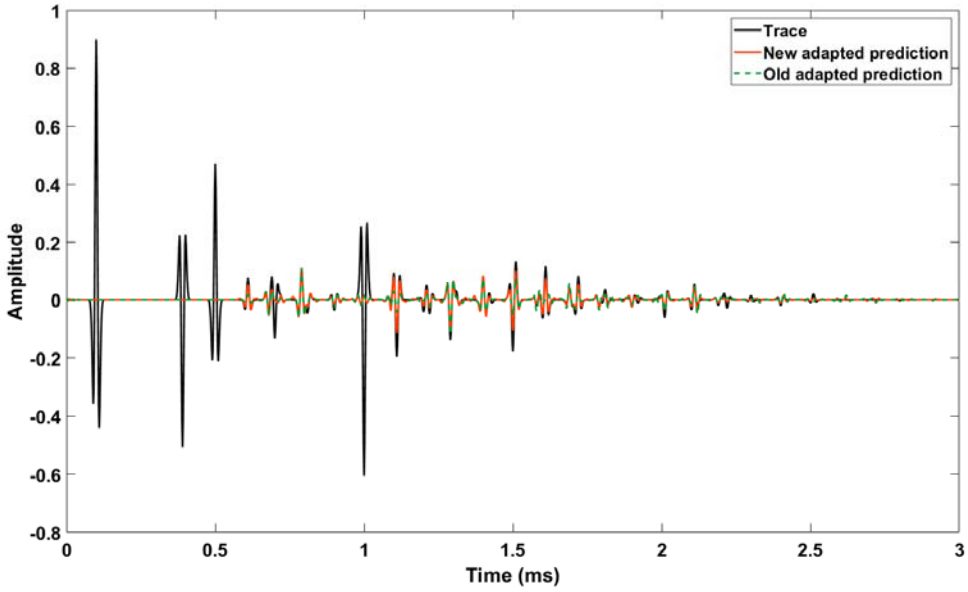

FIG. 1. One-dimensional seismic trace from a lossy medium, with new and old adapted predictions. Gain has been applied to help visualization. Several multiples with transmissions through the lossy layer have been substantially underestimated in the original prediction, but corrected when using the downward-generator domain adaptation approach.

Full-waveform inversion uncertainty analysis with null-space shuttles

Scott Keating* and Kris Innanen

ABSTRACT

Full waveform inversion is an effective tool for recovering subsurface information, but quantification of confidence in this information can be very difficult. Uncertainty in a global sense is ever present when using local optimization, preventing the calculation of an absolute uncertainty. Even when considering local uncertainty, the large dimensionality of the problem means that feasible, intelligible confidence metrics are generally limited to providing a scalar description of confidence for each variable while a vector is properly required. Fortunately, complete characterization of uncertainty is seldom necessary from an applications perspective. More often, the uncertainty in a specific aspect of the inversion is important (for instance, confidence in a recovered anomaly). Here, we investigate the use of nullspace shuttles to characterize the maximal change in a chosen model direction which can be achieved without altering the objective function. This provides a quantification of our uncertainty as defined by the objective function in this direction.

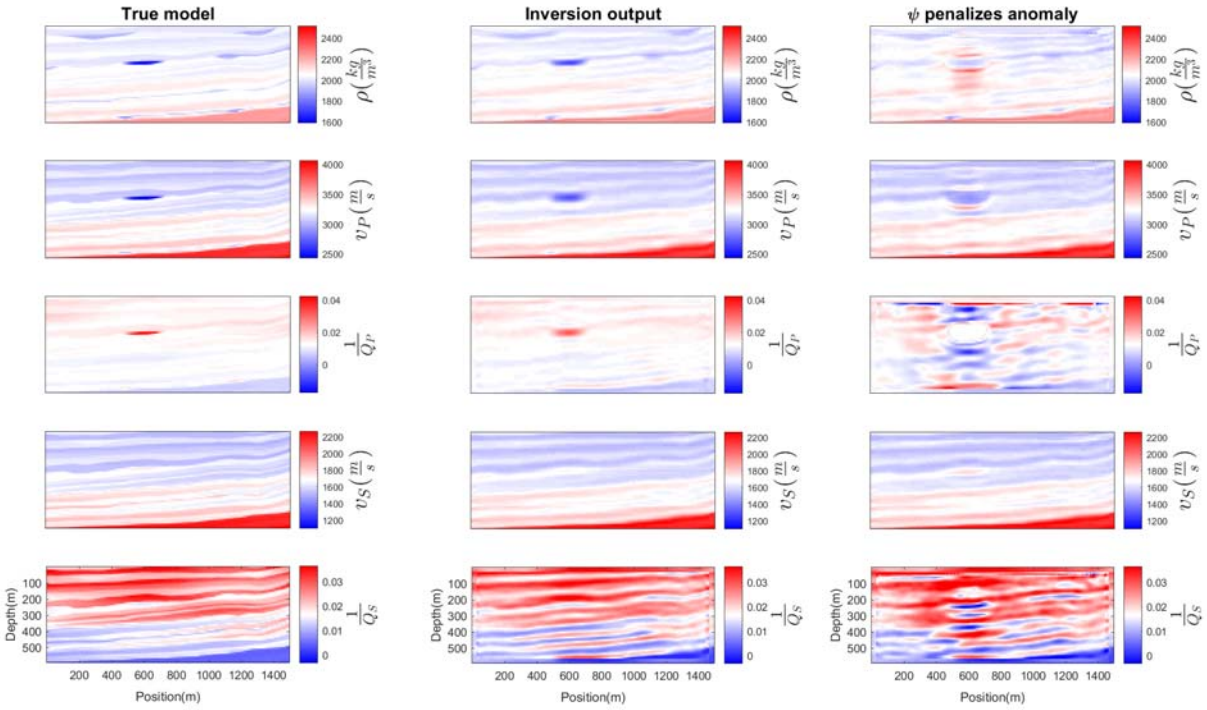

FIG. 1. True model (left), inversion result (center), and equivalent-objective model (right) for visco-elastic synthetic test. The model on the right has the same FWI objective function as the center but has been optimized to eliminate the anomaly. The successful removal of density and Q_P anomalies represents low confidence in these variables, while the persistence of the v_P anomaly suggests high confidence.

Inner-loop penalty terms for cross-talk reduction in viscoacoustic full waveform inversion

Scott Keating and Kris Innanen

ABSTRACT

Inter-parameter cross-talk, where physical properties are confused with one another, is a major concern in multi-parameter full waveform inversion. Cross-talk is difficult to prevent, not least because it is difficult to identify in a recovered model. Certain modes of cross-talk, however, may be more evident in the model updates used in the inversion. We propose penalizing evidence of cross-talk in the model updates within a truncated Newton optimization. We test this approach to penalize cross-talk between v_P and Q_P in an anelastic inversion. We find that an update penalty term can be effectively included in a truncated Newton strategy, but that the penalty terms we investigate are poor measures of cross-talk.

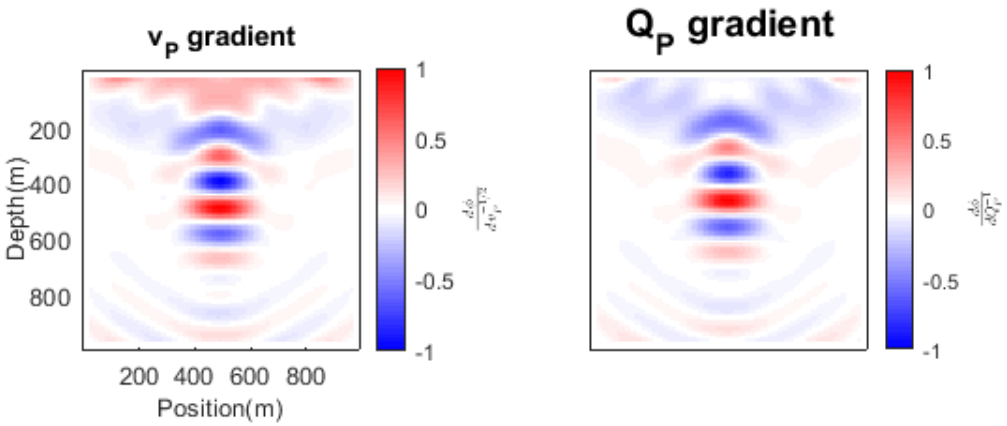

FIG. 1. Gradient of FWI objective function with respect to squared P-slowness (left) and $1/Q_P$ (right) for a simple synthetic test. Displayed amplitudes are relative to maximum amplitude for each parameter. These gradients share largely the same structure, but the $1/Q_P$ gradient is shifted closer to the sources and receivers at the surface. Because of this shift, this structural matching does not represent a geologically reasonable relation between the gradients. We propose penalty terms to prevent cross-talk evidenced by similar relations between v_P and Q_P in possible model updates.

Parameter cross-talk and leakage between spatially-separated unknowns in viscoelastic full waveform inversion

Scott Keating and Kris Innanen

ABSTRACT

Elastic and attenuative effects play a major role in the determination of wave amplitudes and phases observed at seismic sensors. Viscoelastic full waveform inversion (FWI) has the potential to recover much of the information content of measured seismic data by simultaneously accounting for these effects. However, viscoelastic FWI introduces a set of new challenges, especially the phenomenon of cross-talk. Cross-talk is typically characterized through analysis of the radiation patterns of point scatterers; however, the point scatterer model is not well suited to viscoelastic FWI, because: (1) attenuation introduces a significant potential for cross-talk between variables distant from one another in space, and (2) interpreting the effect of frequency and phase dependence on the radiation patterns of point scatterers is not straightforward. Cross-talk can alternatively be analyzed numerically, but here some uncertainty is introduced regarding the generality of the conclusions. We present and examine a numerical approach to assessing viscoelastic cross-talk based on differences between various model residual quantities. With it, we observe strong cross-talk both between velocity and Q variables, and into density for a variety of acquisition geometries. Of particular note is our characterization of the tendency for Q variables to leak into elastic variables from which they are spatially separated. This type of cross-talk is not easily characterized through the use of radiation patterns.

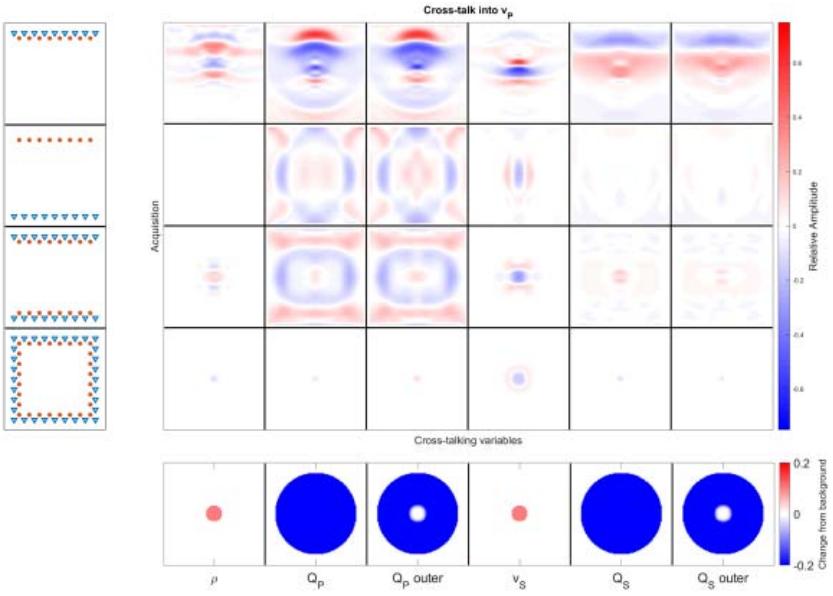

FIG. 1. Cross-talk *from* the variables below the x-axis *into* v_P^{-2} for small, circular elastic scatters and a larger obscuring Q region. Panels show the cross-talk contribution for each of the acquisition geometries illustrated on the left of the y-axis. Cross-talk is largest from all variables in a surface-only acquisition. Cross-talk from Q_P and v_S remains large even for more comprehensive non-complete acquisition scenarios.

Viscoacoustic wavefield reconstruction inversion - obstacles for multi-parameter cycle-skipping strategies?

Scott Keating and Kris Innanen

ABSTRACT

The obstacle of cycle-skipping in full-waveform inversion has led to the development of many non-L_2 objective functions with better convexity properties. While these are effective in their goal of mitigating cycle skipping, they are typically investigated only with a single-parameter inversion formulation. If simultaneous multi-parameter inversion is to be an effective technology, it is important to understand how these objective functions behave when more than one medium property is considered. Here, we investigate the behaviour of one such strategy, wavefield reconstruction inversion, in the case of simultaneous viscoacoustic inversion. We find that prohibitive cross-talk between inversion variables is recovered when adopting this approach.

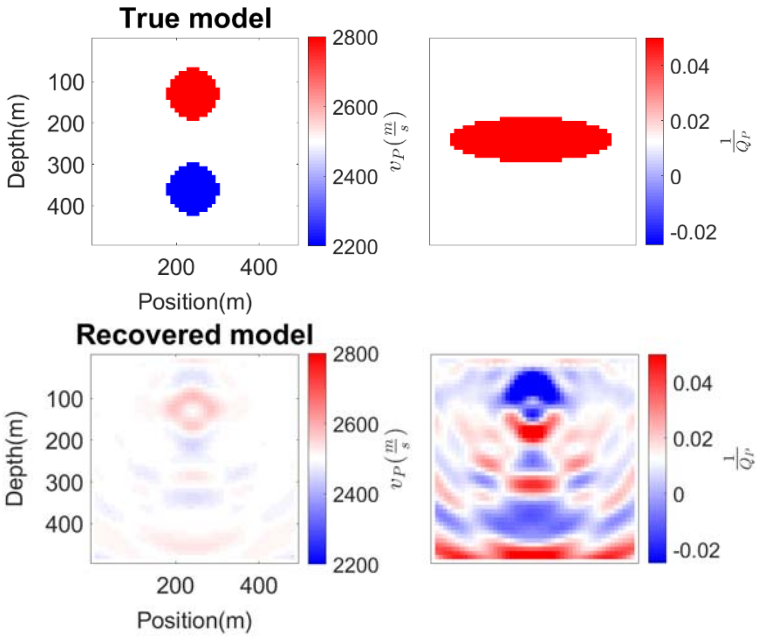

FIG. 1. Top: Example model used for synthetic tests. Inversion began with constant background. Bottom: Wavefield reconstruction inversion result after 300 iterations. Inversion output Q_P values are overwhelmingly dominated by cross-talk. Further, there is poor recovery of the v_P model. This raises concerns for the applicability of extended-model waveform inversion strategies in multiparameter settings.

Gabor multipliers revisited

Michael P. Lamoureux

ABSTRACT

Time-frequency methods have proven to be valuable in seismic data processing as localized Fourier transforms can accurately analyse the nonstationary characteristics of data in response to the non-uniform geology of the region under survey. For instance, Gabor deconvolution by way of Gabor multipliers is an effective way of extending stationary Weiner decon and spectral whitening to the nonstationary seismic domain.

We propose the continuous wavelet transform and its multipliers as an improvement over Gabor methods, using the logarithmically-spaced frequency bins in the CWT to improve resolution and control in the lower frequency range of the seismic signal.

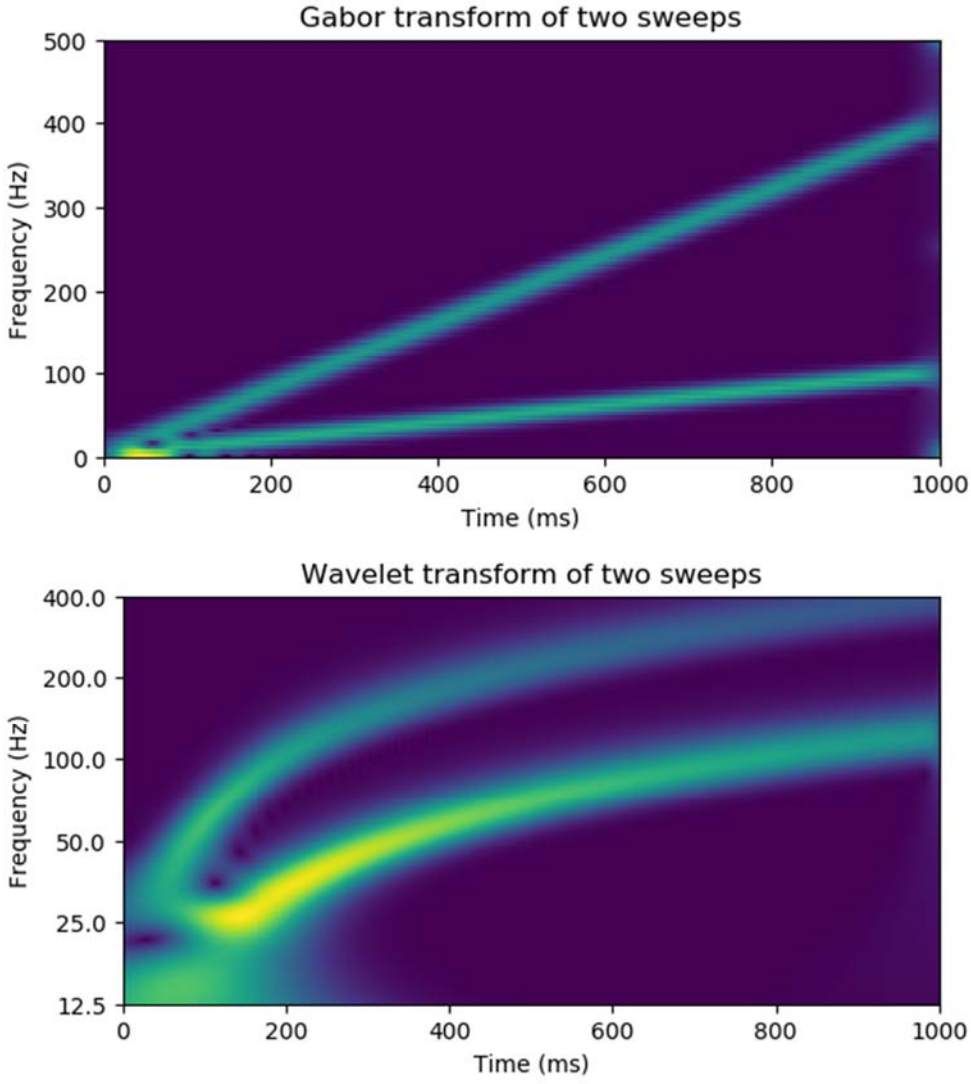

FIG. 1. Comparison of Gabor and Wavelet transforms. Note the resolution at low frequencies.

Review of tomographic methods

Bernard K. Law* and Daniel Trad

ABSTRACT

Classical reflection tomography requires traveltimes to be picked on continuous events on CDP stacks and unmigrated gathers. This can be difficult for noisy data, data with complex structures and for large dataset. PSDM tomography and stereotomography has picking advantage over classical reflection tomography. In addition to traveltimes, stereotomography also uses ray-parameters in the inversion.

Classical reflection tomography

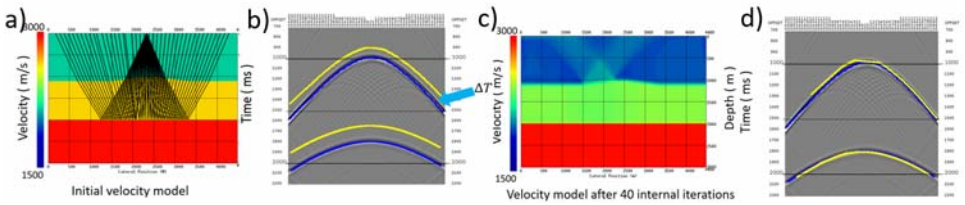

FIG. 1. (a-d) Classical reflection (Bishop 1985) updates the velcoity model by minmizing the differences between the observed reflection times on prestack data and the raytraced reflection times.

PSDM tomography

$$z_m = \sqrt{\gamma^2 z^2 + (\gamma^2 - 1)x^2}, \qquad \gamma = \bar{V}_m / \bar{V}, \qquad \text{Al-Yahya (1989)}$$

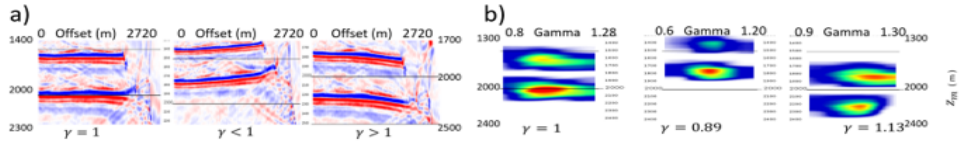

FIG. 2. (a) Residual curvature from common reflection point gathers from prestack migration. (b) Gamma scan using equation from Al-Yahya (1989). Velocity ratios are used to update the velocity along the ray paths (Gray 2000) or used to compute travel time residual for tomography (Stork 1992)

Adjoint stereotomography

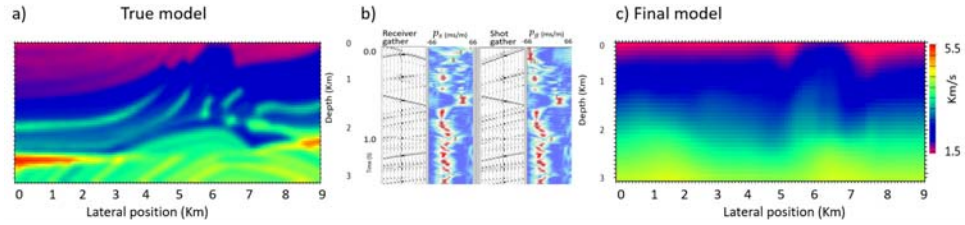

FIG. 3. (a) True velocity model. (b) Synthetic shot gathers, slant-stacks and ray-parameters picks. (c) final velocity after 5 iterations.

Update on DAS and geophone VSP surveys at the CaMI Field Research Station, Newell County, Alberta

Don Lawton, Adriana Gordon, Kevin W. Hall, Michael Hall[1] and Svetlana Bidikhova[1]

ABSTRACT

As part of on-going seismic monitoring at the CaMI Field Research Station (CaMI.FRS), vertical seismic profiles are being recorded unto a 24-level permanent downhole 3-component geophone array as well as helical wound and straight optical fibre for Distributed Acoustic Sensing (DAS). The geophones and fibre are all cemented behind the casing in a 350 m deep observation well. The source was an Envirovibe with a sweep of 10 – 150 Hz over 16 s. Data used for this paper were recorded from 14 source points with offsets from 9 m to 299 m from the VSP well. DAS traces were recorded with a 10 m gauge length with an output trace interval of 0.25 m from 15 m to 338.5 m depth. Advances over previous processing included smoothing DAS first break picks, application of both a median and FK filter to separate and enhance the upgoing energy, and careful assessment of shot statics based on minimizing the error between observed and computed first break travel-times. The velocity model for the VSP CDP transform for offset shots was determined initially from well-log data and the zero-offset DAS data, and then updated through matching computed and observed moveout for offset sources. Having the very near-surface velocities available from DAS data enabled a very robust 1-D velocity model to be established. This also improved VSP-CDP stacks of the borehole geophone data and the two datasets match closely. The final VSP-CDP stack enabled excellent imaging up to nearly 100 m from the VSP well for the DAS data and 64 m for the geophone data.

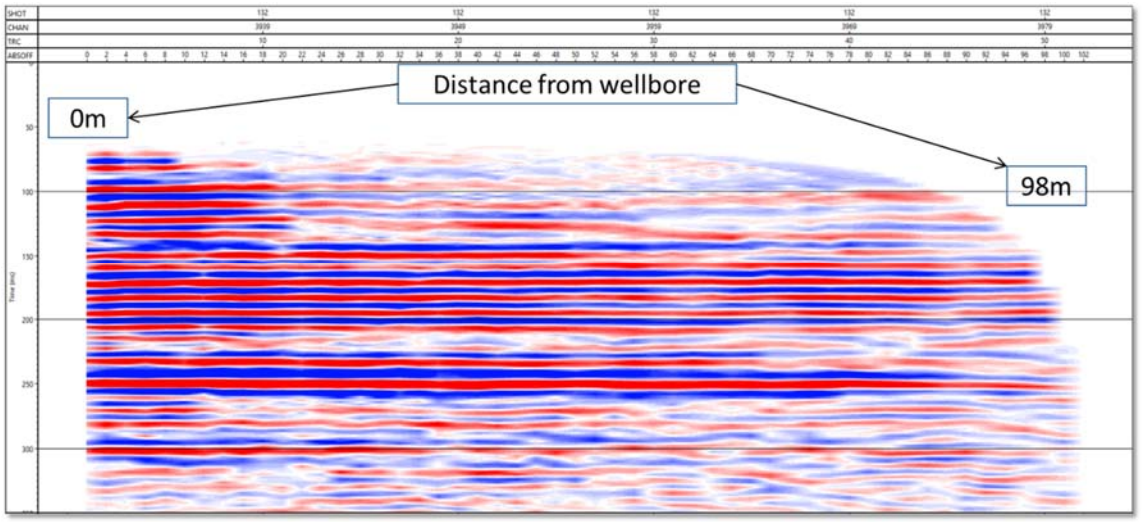

FIG. 1. VSP-CDP stack from walk-away DAS data.

[1] GeoVectra Ltd.

Full waveform inversion with unbalanced optimal transport distance

Da Li*, Michael P. Lamoureux, and Wenyuan Liao

ABSTRACT

Full waveform inversion (FWI) has become a major seismic imaging technique. However, using the least-squares norm in the misfit functional possibly leads to cycle-skipping issue and increases the nonlinearity of the optimization problem. Several works of applying optimal transport distances to mitigate this problem have been proposed recently. The optimal transport distance is to compare two positive measures with equal mass. To overcome the mass equality limit, we introduce an unbalanced optimal transport (UOT) distance with Kullback–Leibler divergence to balance the mass difference. An entropy regularization and a scaling algorithm have been used to compute the distance and its gradient efficiently. Two strategies of normalization methods which transform the seismic signals into non-negative functions have been compared. Numerical examples in one and two dimension have been provided.

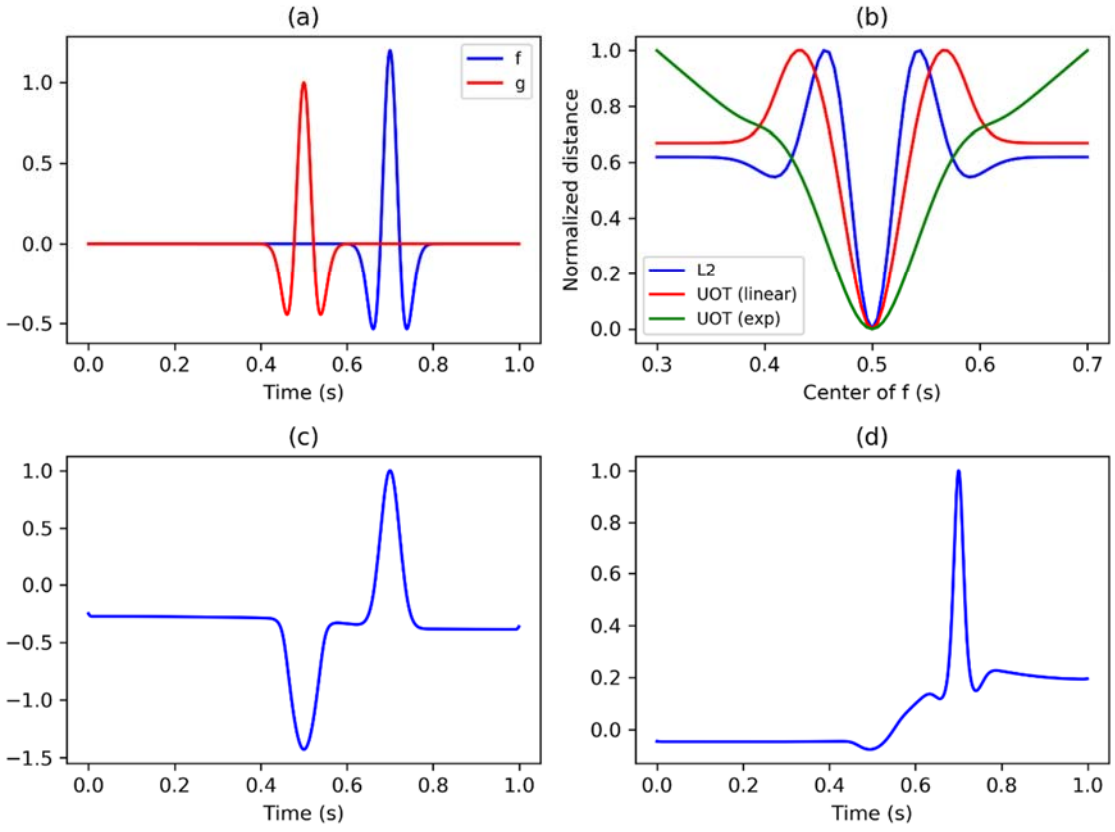

FIG. 1. (a) Two 10 Hz Ricker wavelets f and g. The amplitude of f is 1.2 times of g. (b) Fix g as reference signal, we move the center of f from time 0.3s to 0.7s. The difference between f and g has been compared using L2 distance, UOT distance with linear normalization and UOT distance with exponential normalization. (c) Adjoint source of UOT distance with linear normalization. (d) Adjoint source of UOT distance with exponential normalization.

First-Order qSV-Wave Propagator in 2D VTI Media

He Liu and Kris Innanen

ABSTRACT

The propagation of elastic waves in formations has been widely investigated in the development of seismic exploration. In a typical transversely isotropic medium (e.g., VTI medium), qP- and qSV-waves are intrinsically coupled as described in elastic wave equations. Therefore, coupled qP-wave energy will inevitably contaminate the imaging results from performing elastic reverse time migration (ERTM) and imaging algorithms to qSV-mode waves. Other than directly separate qS-mode waves from full elastic waves in anisotropic media, some researchers have tried to find an alternative way to solve it by the forward simulation of pure-qSV-mode waves. In this study, we propose a first-order wave propagator of pseudo-pure-qSV-mode wave in 2D heterogeneous VTI media, which can be easily employed for the simulation of qSV-mode wave propagation with staggered-grid finite difference scheme. This propagator will directly suppress qP-mode wave energy through projecting the wavefields onto isotropic references of local polarization direction. By further correction of projection deviation of simulated wavefield components, residual qP-waves will be eliminated completely and separated scalar pseudo-pure-qSV-mode waves can be achieved. We have performed the algorithm to isotropic medium, VTI media with weak/strong anisotropy, a two-layer VTI model and part of heterogeneous SEG/Hess VTI model, the synthetic results demonstrate the validity and feasibility of this algorithm. In addition, the more efficient and more stable first-order Hybrid-PML can be directly implemented in this staggered-grid finite difference algorithm, which shows better performance in the wavefield propagation simulation in VTI media with strong anisotropy.

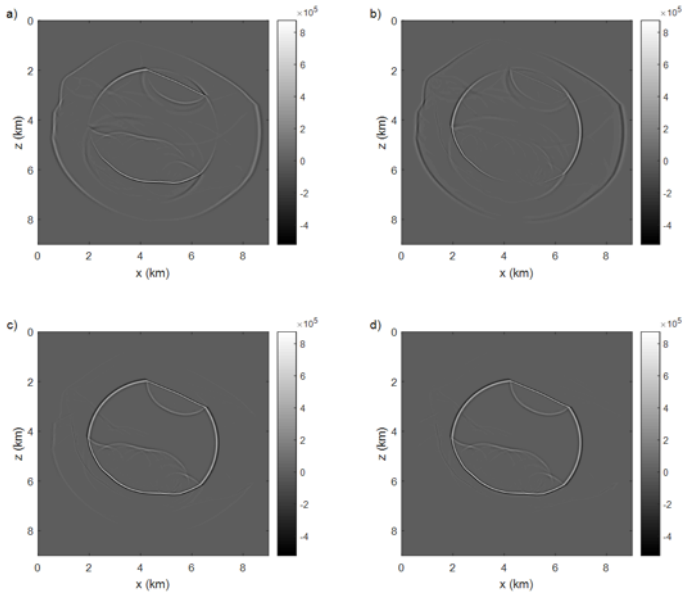

FIG. 1. The synthetic wavefields in SEG/Hess VTI model: a) x- and b) z-component simulated by first-order pseudo-pure-mode qSV-wave equations; c) pseudo-pure-mode scalar qSV-wave field; d) separated scalar qSV-wave field.

Ambient noise correlation study at the CaMI Field Research Station, Newell County, Alberta, Canada

Marie Macquet* and Don C. Lawton

ABSTRACT

We recorded passive continuous seismic data at the CaMI Field Research Station to study the feasibility of using ambient noise correlation method as an additional tool to monitor and verify secure storage of the injected CO_2. In this paper, we focus on two aspects: (1) the near surface tomography, using 112 stations along the 1.1 km trench and (2) the long term monitoring of the velocity change using continuous recording since October 2014 on 7 broadband stations. Due to the frequency range of the geophones used for the tomography part, the investigation depth remains shallow (up to 50 m depth). Nevertheless, a good near-surface velocity model remains important for active seismic processing. Figure 1 shows the V_S model obtained with ambient noise correlation method. It is similar to the one obtained from an active shear seismic source study (bedrock depth and V_S range). The daily correlations (Figure 2) between 2 broadband stations show good coherency. Velocity variation between the daily correlations and the reference is computed to better understand the impact of the environmental changes on the Green's function reconstruction.

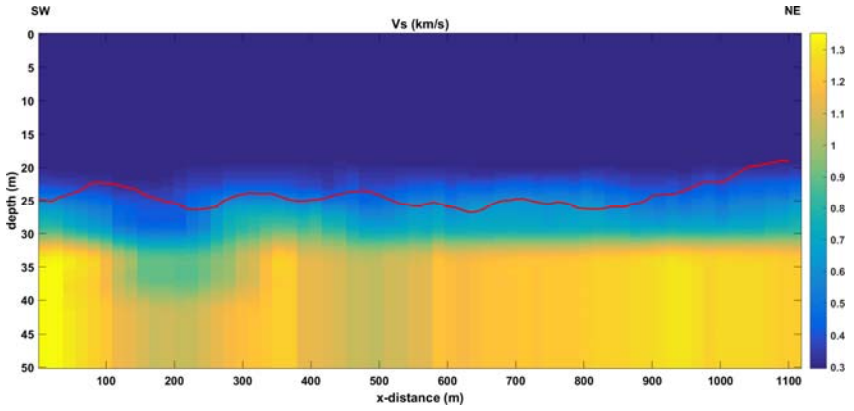

FIG. 1. S-wave velocity model recovered from ambient noise correlation method. Red line is the bedrock depth from shear-source study (Isaac and Lawton, this volume).

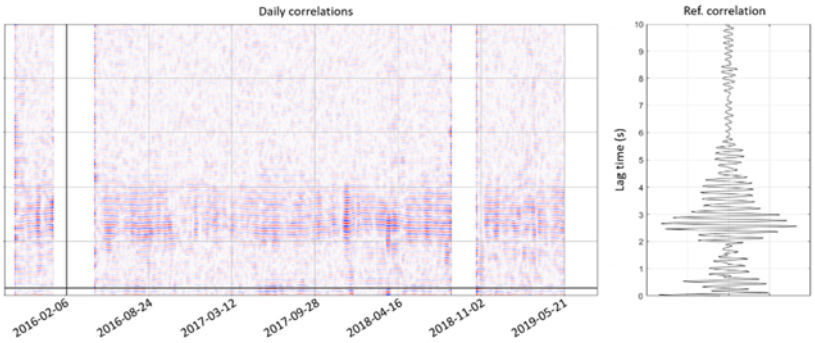

FIG. 2. Left: 4 years of daily correlations between two broadband stations (FRS3 and FRS4). Right: stacked correlation.

RTM of a distributed acoustic sensing VSP at the CaMI Field Research Station, Newell County, Alberta, Canada

Jorge E. Monsegny*, Daniel Trad, and Don C. Lawton

ABSTRACT

We applied a reverse time migration (RTM) algorithm to distributed acoustic sensing (DAS) data from a walkaway vertical seismic profiling (VSP) acquisition at the CaMI Field Research Station at Newell County, Alberta, Canada. The RTM algorithm used a system of coupled first degree differential equations for pressure, vertical and horizontal particle velocities. As DAS data measurements are usually strain rate, we transformed them to vertical particle velocity before the RTM algorithm backpropagated them. We tested the techniques of Daley et al. (2016) and Bóna et al. (2017) to do this transformation. We also tested the RTM with the original DAS data. Apart from a polarity reversal, there were no important differences between the different RTM tests. In addition, we migrated geophone data from the same VSP acquisition for comparison and found a similar imaging quality.

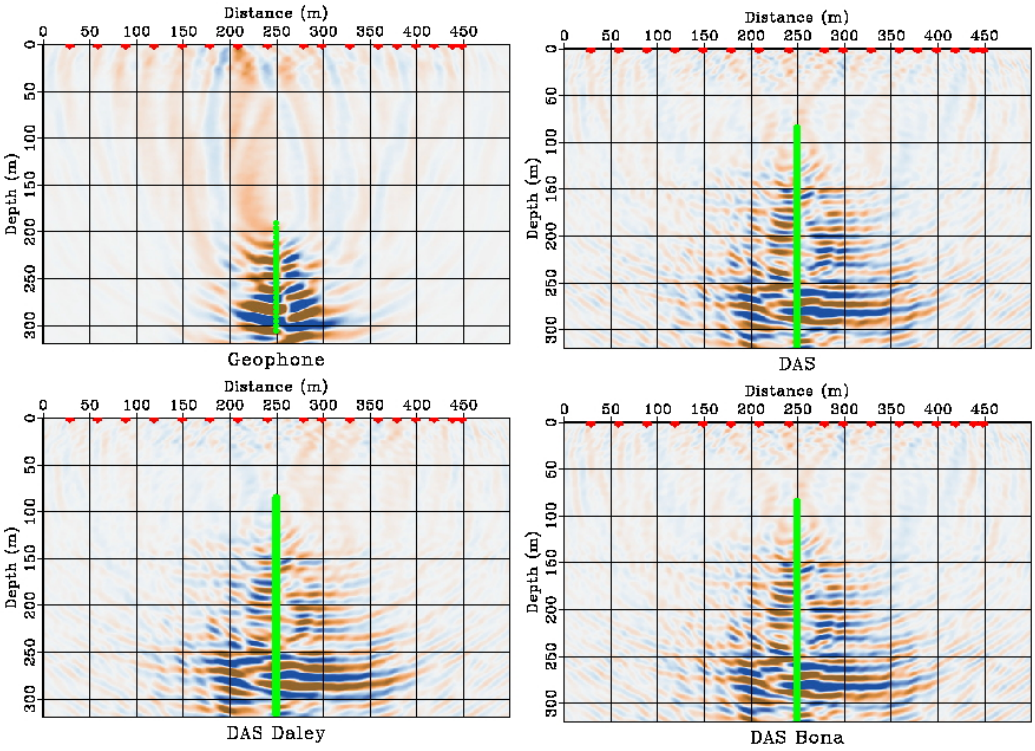

FIG. 1. Top row left is the RTM from 24 vertical geophones located inside the well (green dots) between 190m and 305m deep every 5m and 17 source positions placed at the surface (red crosses). Top row right is the RTM from a DAS fibre located in the well (green line) between 85m and 317m deep. It uses the same sources of the previous figure. The DAS data was not transformed before being used in the RTM, i.e. strain rate was backpropagated by the migration algorithm. Botton left uses the same DAS and sources configuration but transforms the strain rate measurements into particle velocity using the technique of Daley et al. (2016). Bottom right also transforms DAS measurements to particle velocity but it uses the technique of Bóna et al. (2017). Laplacian filtering was not applied to any figure because it did not produce any noticeable effect.

Deblending using convolutional neural networks

Zhan Niu* and Daniel Trad

ABSTRACT

Machine learning has been a booming subject in computer science and its applications have been made in various subjects including geophysics. Convolutional Neural Networks (CNNs) have great potential for solving image processing problems like denoising and interpolation. Deblending, considered as an underdetermined denoising problem, falls into this category. In this report, we use CNN to replace the deblending operator and its performance is analyzed. We use a 4-layer U-Net to perform deblending on synthetically blended shots from a wedge velocity model with point scatterers. We test out different hyper-parameters and the trained model could successfully remove the noise and preserve diffractions from the scatterers with some tolerance. The generality of the model is evaluated by testing the model on an easier 2-layer velocity model. The model can successfully identify and recover most part of the primaries but fails to deal with some interferences and leaves them muted.

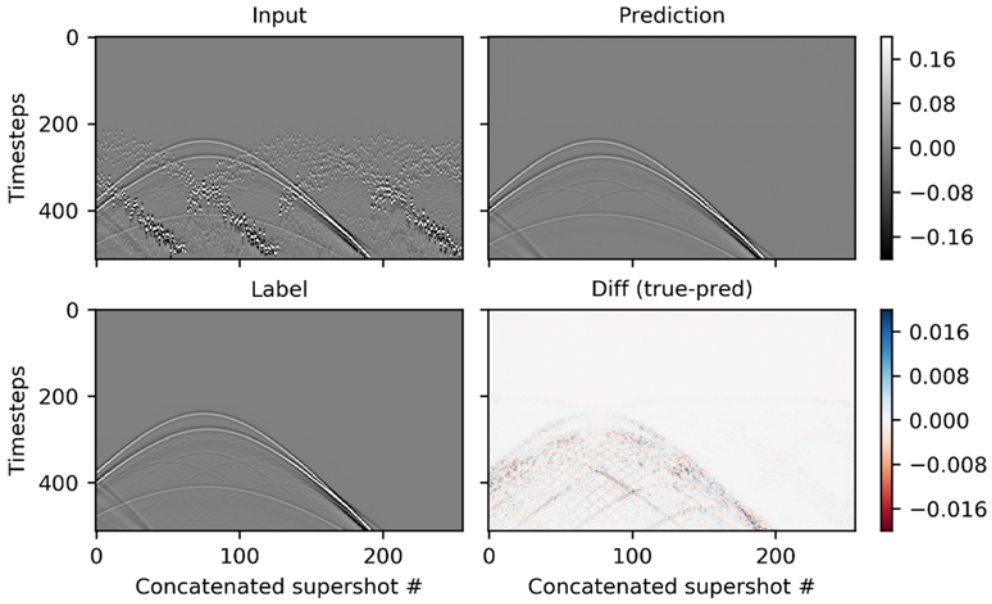

FIG. 1. The prediction and label for a receiver gather in the validation set. All three grayscale pictures have the same scale. The picture in the upper right shows the prediction made by the model and the picture in the bottom right shows the difference between the prediction and the label with a smaller color scale.

Machine learning experiments on velocity extraction from migration images

Zhan Niu and Daniel Trad

ABSTRACT

In full waveform inversion (FWI), the update of velocity is obtained by calculating the gradient of the misfit between recorded and predicted data, which is defined by the cross-correlation of the reverse time of receiver wavefield and source wavefield. Benefits can be achieved by solving a direct non-linear mapping between the correlation and model update. In this report, we train a fully connected neural network with residual blocks which allows migrated images to be directly mapped into velocity models. The input images and the true velocity model comes from reverse time migration results on randomly generated 4-layer models. The training is performed with ADAM optimizer combined with L1/L2 norms as the cost function. Performance and convergence of the neural network with different hyper-parameters are also investigated systematically. We have tested the trained model with different synthetic inputs. Results show the that the trained network is relatively model dependent which performs well on the validation set but does a poor job on datasets that come from different distributions.

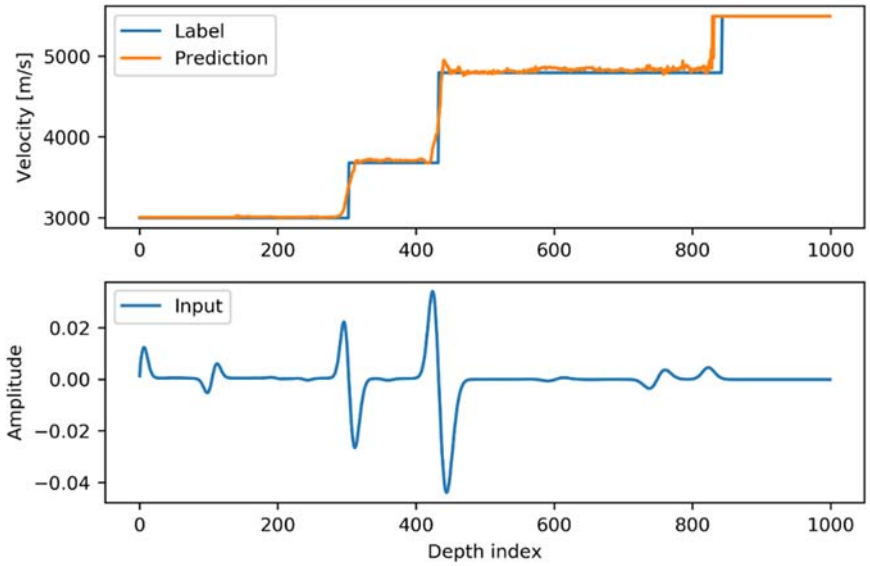

FIG. 1. The blue line in plots on the top is the true model while the orang line refers to the prediction made by the model. The bottom plot shows the migration image fed to the model. All interfaces except the last one have been successfully identified.

Comparison of different surface wave dispersion inversion methods

Luping Qu and Kris Innanen

ABSTRACT

Multichannel Analysis of Surface Wave (MASW) inverts the S wave velocity using the Rayleigh dispersion curve. It has three steps: field data acquisition, dispersion analysis, inversion analysis. Due to its robustness and simplicity, it is the most widely used method to characterize the near surface velocity. Factors influencing the method's accuracy are analyzed, and the determination method for the initial input parameters is given. Advantages and limitations of MASW are introduced in this paper. For modeling tests, we used SPECFEM to generate synthetic data, using the misfit of the generated dispersion curve and picked dispersion curve of the synthetic data to update S wave velocity. The least square Gauss-Newton inversion method is adopted to minimize the misfit. The damping parameter and stability parameter of the inversion are tested. In addition, global optimization methods like Simulated Annealing and Monte Carlo using Markov Chain were applied to simple layered models.

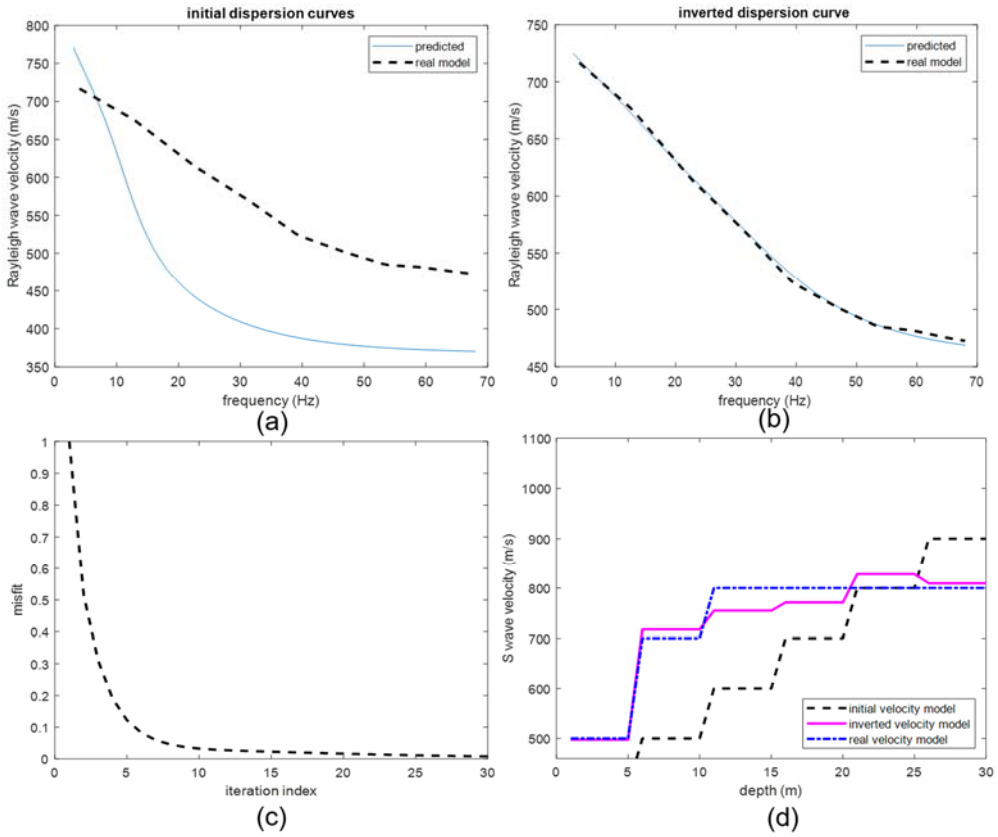

FIG. 1. Gradient based inversion results for a three-layered model with unknown layer number. (a) Initial observed and predicted dispersion curves. (b) Observed and predicted dispersion curves after inversion. (c) Misfit with iterations. (d) Inversion result.

Trans-Dimensional multimode surface wave inversion of DAS data at CaMI-FRS

Luping Qu*, Jan Dettmer and Kris Innanen

ABSTRACT

Due to the limited research on the combined utilizations of multimodal phase velocities in surface wave dispersion inversion, this study implements a trans-Dimensional surface wave dispersion inversion by using the multimodal phase velocities of the Rayleigh wave, and applies it to surface Distributed Acoustic Sensing (DAS) data. The joint principle of multiple modes combination in a stochastic sense is explained in detail in this work. A thorough spectral analysis and error estimations on DAS data are displayed and a new mode separation method called dispersion compensation is adopted for clear dispersion curves picking. Multimodal phase velocity dispersion curves are extracted from the densely sampled DAS data, and then utilized for a multimode phase velocity trans-Dimensional inversion. Underground information inferred by the phase velocity is demonstrated, better results through incorporating higher mode Rayleigh wave phase velocity are shown. Tests are carried out on synthetic models and field DAS data in Containment and Monitoring Institute-Field Research Station. Results of synthetic models are consistent with the theoretical expectations, and results of real data is in excellent agreement with known geology features. A better characterization of shallow area is revealed compared with other research results.

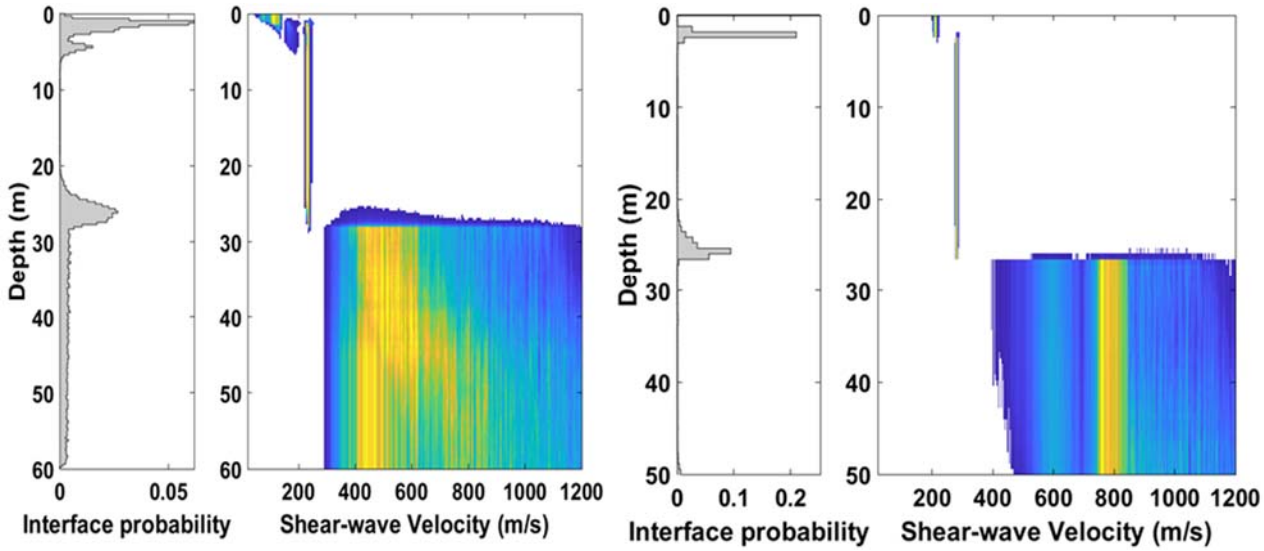

FIG. 1. Trans-dimensional results for DAS data. (a) Vs inversion results for fundamental mode dispersion curve. (b) Vs inversion results for multimode dispersion curves.

A numerical comparison of seismic inversion, multilayer and basis function neural networks

Brian H. Russell[1]* and Laurence R. Lines

ABSTRACT

In this presentation, a numerical example is used to illustrate the difference between geophysical inversion and several machine learning approaches to inversion. The results will show that, like inverse geophysical solutions, machine learning algorithms have a definite mathematical structure that can be written down and analyzed. The example used in this study is the extraction of the reflection coefficients from a synthetic created by convolving a dipole reflectivity with a symmetric three point wavelet. This simple example leads to the topics of deconvolution, recursive inversion, linear regression and nonlinear regression using several machine learning techniques. The first machine learning method discussed is the multi-layer feedforward neural network (MLFN) with a single hidden layer consisting of two neurons. The other two methods which are discussed are the radial basis function neural network (RBFN) and the generalized regression neural network (GRNN). As will be shown, all three of these networks involve different basis functions. In the MLFN the basis function is the sigmoidal logistic function and in both RBFN and GRNN the basis function is the Gaussian. However, for RBFN the weights are computed using a least-squares algorithm and in GRNN the weights are computed "on-the-fly" using the observed data. The MLFN algorithm is iterative and the key parameters are the initial random weights, the learning rate and the number of iterations. The RBFN and GRNN are not iterative and the key parameter in both methods is the width of the Gaussian, or sigma factor. Figures 1 (a) to (d) below show a comparison of the results of linear regression and the three machine learning algorithms. In all four figures, the horizontal axis represents the computed seismic amplitudes and the vertical axis represents the desired reflection coefficients. The black circles show the four training values, and the solid line shows the fitting function from the linear or nonlinear regressions. For the MLFN result, 10,000 iterations and a learning rate of 0.2 were used, and for both the RBFN and GRNN results a sigma factor of 0.5 was used.

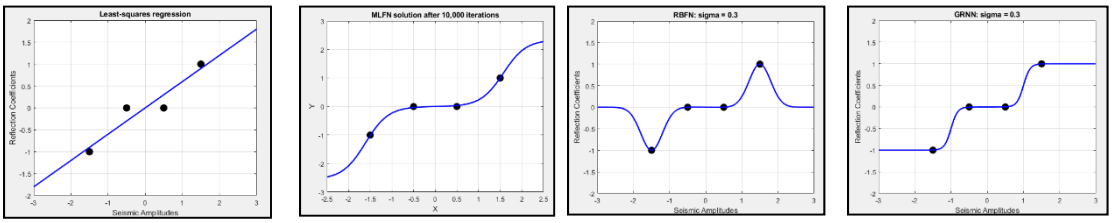

FIG. 1. The above figures show predicted reflection coefficient versus seismic amplitude for (a) linear regression, (b) the feed-forward neural network with 10,000 iterations and a learning rate of 0.2, (c) the radial-basis function neural network with sigma = 0.5 and (d) the generalized regression neural network with sigma = 0.5, where the black circles are the training points and the solid line is the fitting function.

[1] HampsonRussell, A CGG GeoSoftware Company, Calgary, Alberta, brian.russell@cgg.com

Migration and demigration deblending in receiver domain

Ziguang Su and Daniel Trad

ABSTRACT

Some seismic acquisitions have more sources than receivers. Under that circumstance, receiver domain Revere Time Migration/RTM saves computation time compared with shot domain RTM. The reciprocity algorithm of wave propagation can be derived from the principle of reciprocity, which can be utilized in the exchange of source and receiver locations for the seismic acquisition data. Receiver domain RTM can also be applied in deblending for simultaneous sources data/blended data, in which dithering can be utilized for blended data onto the receiver domain. Therefore receiver domain RTM could be a method of migration and demigration to deblending.

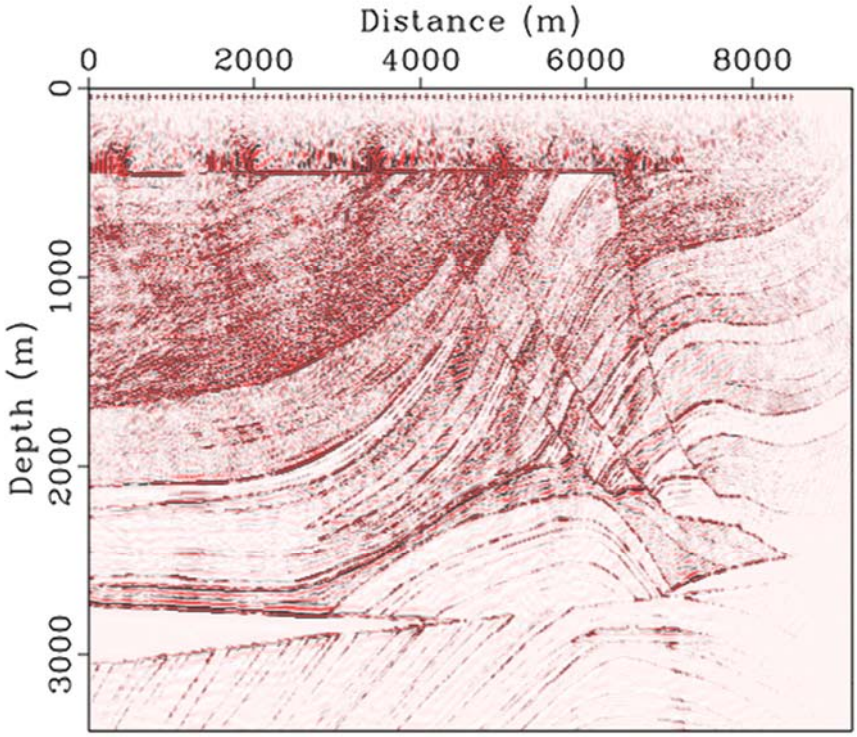

FIG. 1. The result of RTM in marmousi model.

A Madagascar package for deblending in multiple flavours

Daniel Trad*

ABSTRACT

Simultaneous acquisition is a very cost-effective approach that reduces the cost of seismic information in both marine and land settings. Its main difficulty is the processing of the resulting seismic data, which requires shot separation or deblending, very early in the signal processing chain. There are several approaches for deblending seismic data: denoising, inversion and physical transforms:

Denoising: data are expanded along the shot axis by the number of blended shots and shifted along the time axis following time delays applied during acquisition. This process, called "pseudo-deblending", has the effect of making seismic events coming from one of the shots coherent and the events coming from the other shots incoherent. This is visible only on seismic domains where groups are formed by different shots. The incoherent energy is removed by denoising methods that can account for residual outliers.

Inversion: all groups are simultaneously inverted by using a transform with many operators acting in parallel, chained to a blended operator. These groups are all fitted (predicted) by the combination of transform panels. Model sparseness is used to eliminate cross-talk across transform panels.

Physical transforms: use physics to map the blended data to the correct physical space to which they belong to. Once the correct physical space is built, shots can be predicted in the deblended (extended) space.

In this report, we will see how the three approaches are related. Converting between different techniques can be seen as redefining the transform and moving the transform from outside to the inside of the optimization algorithm.

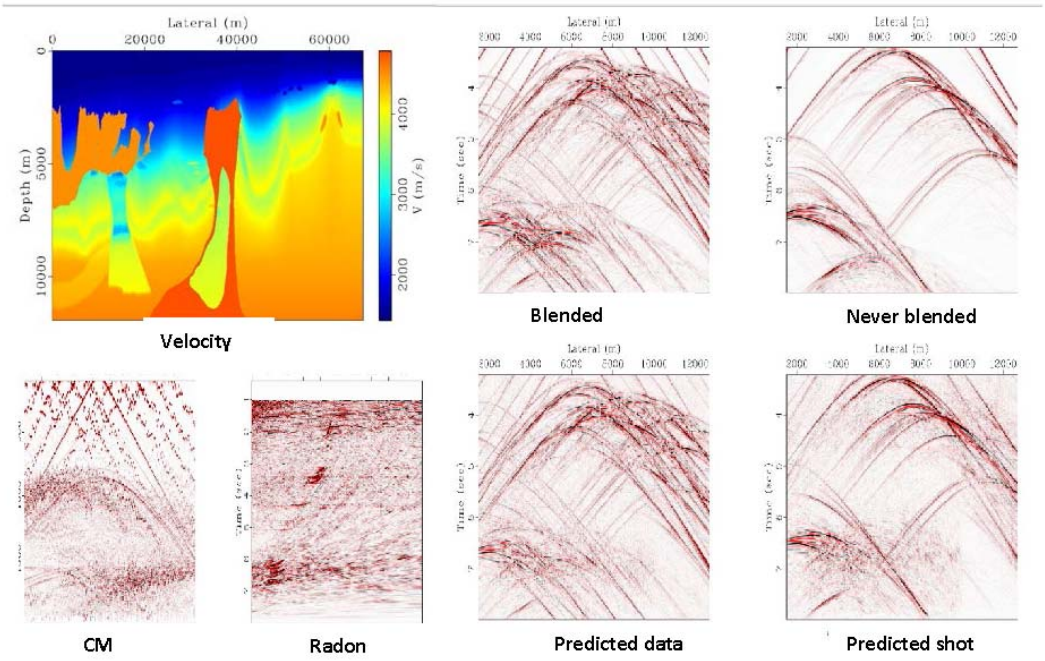

FIG. 1. Deblending by inversion 100 shots from the left side of the BP2004 model, blended in groups of 5 supershots. The inversion transform is hyperbolic time domain Radon.

Integrated Interpretation: Using seismic data to de-risk the Duvernay

Ronald M. Weir*, Laurence R. Lines, and Don C. Lawton

ABSTRACT

Development of a resource play such as the Duvernay Formation is subject to intrinsic risks. These may include the risk of incurring additional costs due to an induced seismic event, or risks associated with unexpected thermal maturity, which can determine the value of the processed hydrocarbons (dry gas vs. condensate). These two risks may be related, as the presence of basement faulting may influence the heat flow from the basement, causing local variations in thermal maturity. The presence of basement faulting may also increase the risk associated with induced seismicity, whereby pre-existing faults are reactivated during the course of well treatment. Interpretation is complicated by the variable depositional environment for the Duvernay marine shale; an off-reef depositional system includes mechanisms such as contourite deposition, turbidity/mass flow, and in-situ biological carbonate precipitation, thereby creating variances in total organic hydrocarbon content. Transtensional faulting caused by deep seated strike-slip faults may be reactivated during a completion program, rather than induced hydraulic fractures. Combining the microseismic and reflection data and displaying the data in depth allows the joint interpretation of reflection seismic and microseismic data. A geological picture is constructed by visualizing microseismic hypocenters in a chair plot with reflection surfaces and depth slices. These can be used to determine best practices for the future location and design of horizontal treatment wells.

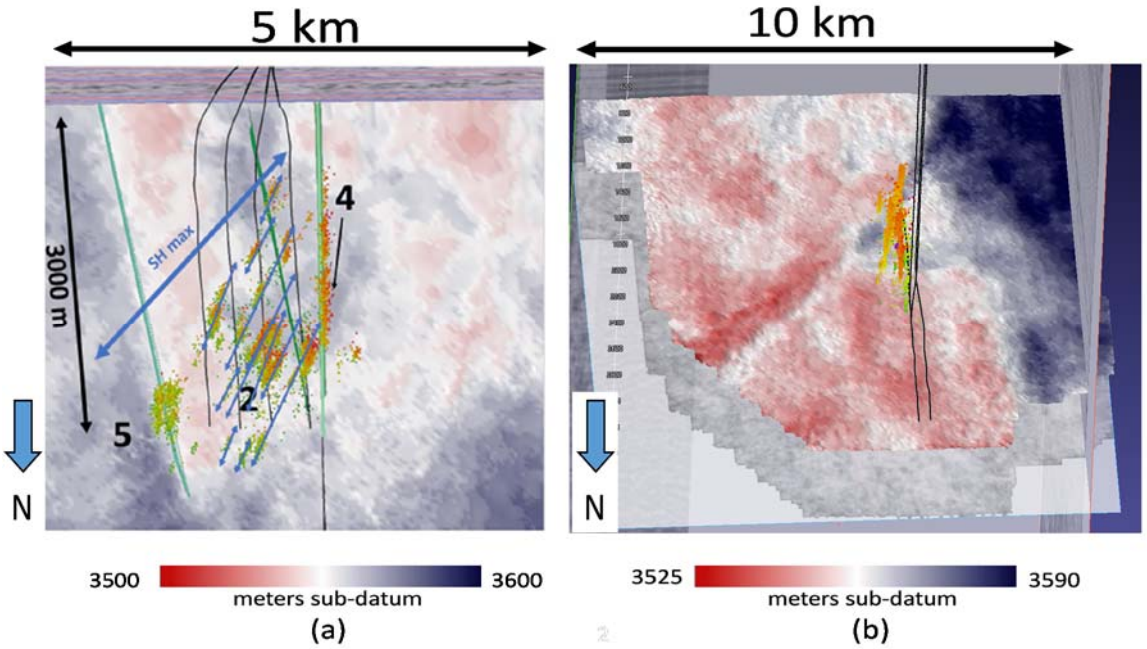

FIG. 1. Swan Hills Formation Depth converted maps for the two adjoined study areas, shown as chair plots. Microseismic events generated by the Duvernay Formation completion program are plotted as points within the seismic volume. The microseismic events within the Duvernay Formation tend to follow pre-existing faults, NNE trending (a), and N-S (b). SH max is 43° N in both areas.

Microseismic and time reversal physical modeling

Joe Wong*, Hongliang Zhang, Kevin L. Bertram, and Kris Innanen

ABSTRACT

We have conducted two physically-model experiments: (a) a microseismic survey to acquire data for hypocenter location through an HTI layer, and (b) an acquisition of data to illustrate propagation reciprocity, time reversal, and wave focusing. Hypocentre location can be done via optimization algorithms and ray tracing using the Byun equations for describing HTI velocities. Time reversal is demonstrated by reversing the roles of sources and receivers and firing the reversed receivers with the proper delay times to focus wave energy at reversed source location in 2D/3D. The data are available to CREWES personnel and sponsors for further analysis.

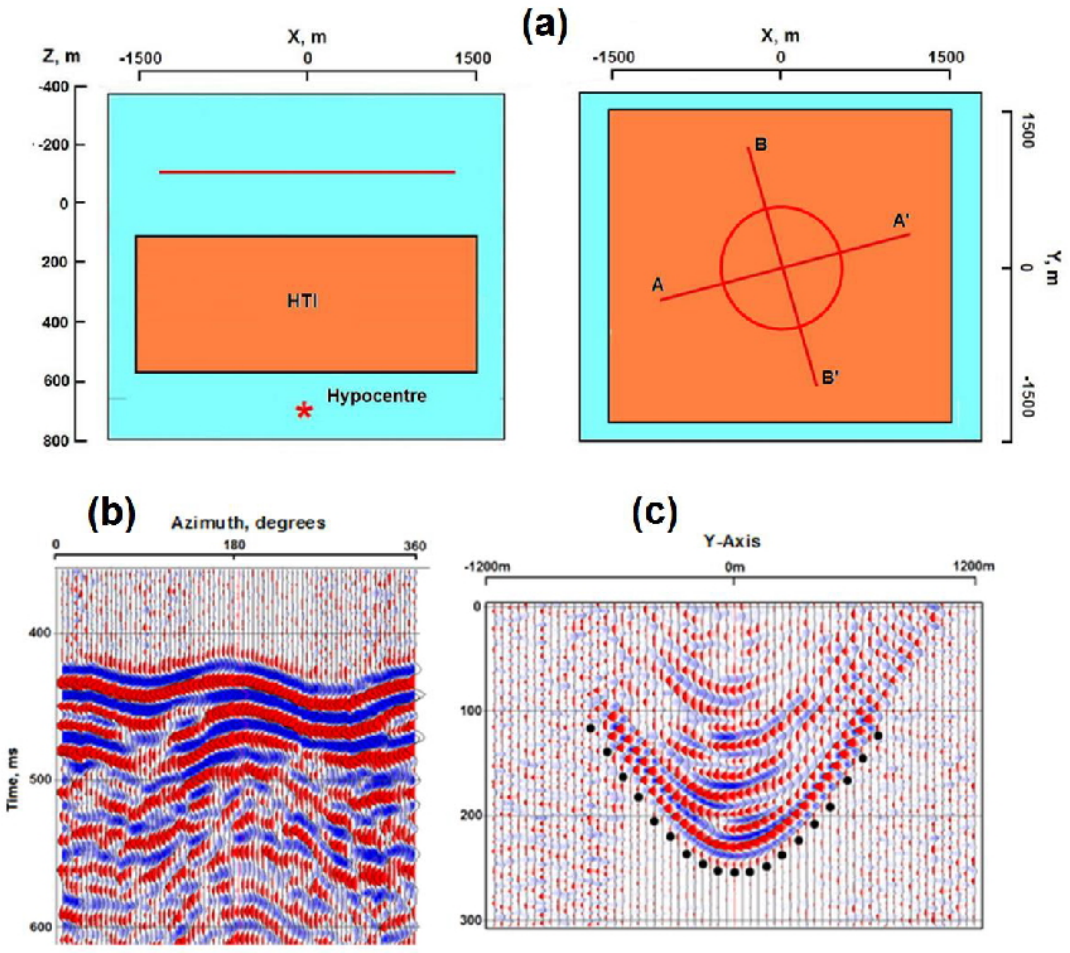

FIG. 1. (a) Schematic of physical modeling of microseismic acquisition on crossed and circular receiver arrays. (b) Microseismograms recorded on the circular array with radius 500m and 5 degree increments. (c) Mirrored, windowed, and reversed-time traces from the time reversal experiment. Black dots represent delay times for reversed firing, i.e., using surface receivers in (a) as sources and the subsurface source (hypocentre) as a receiver.

Physical modeling of seismic illumination and SWD

Joe Wong, Hongliang Zhang, Kevin L. Bertram, Nasser Kazemi, and Kris Innanen

ABSTRACT

We have conducted physical modeling to show that surveys using surface-only seismic sources and receivers can result in shadow zones (caused by an upper high-velocity blocking structure) in the illumination of deep target zones. The deficient illumination may be mitigated by seismic while drilling (SWD) acquisition, wherein we record vibrations generated by drill-bits at depth interacting with rock. Simulating this in a physical modeling experiment requires that we be capable of producing complex source waveforms to drive piezoelectric transducers located below the surface. So far, we have recorded the subsurface-source seismograms only with impulsive source waveforms.

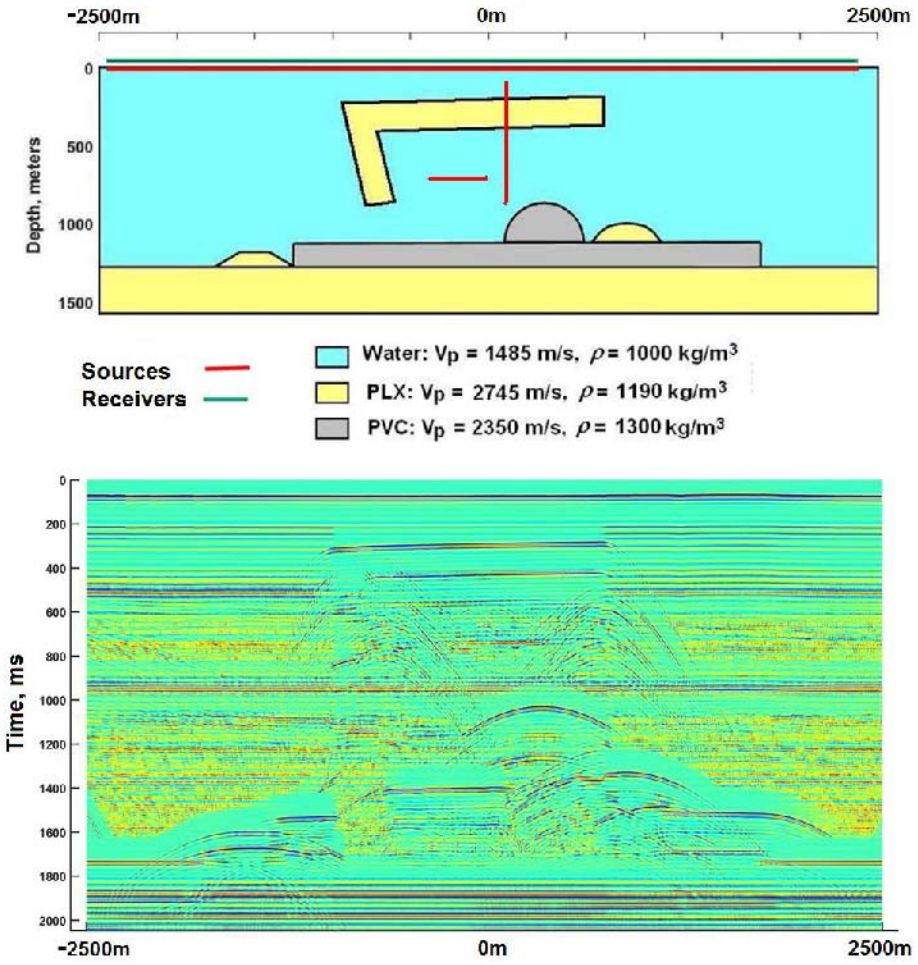

FIG 1. Top: A physical model for investigate seismic illumination and its mitigation by SWD acquisition. Lines at 0m represent surface locations of sources and receivers. Other red lines represent subsurface source locations. Bottom: AGC plot of unprocessed impulsive seismograms from a high-resolution zero-offset survey over the physical model. Trace spacing is 5m.

Interpolation through machine learning

Hongliang Zhang*, Amr Ibrahim, Daniel Trad, and Kris Innanen

ABSTRACT

Inspired by the image super-resolution problem, a CNN-based residual dense network (RdNet) is utilized to interpolate the missing seismic traces based 2D synthetic seismic data. For the sake of comparison, interpolations are also implemented with previously proposed residual network (ResNet) and minimum weighted norm inversion (MWNI). As demonstrated by a series of synthetic experiments in this study, the contiguous memory mechanism, residual learning and feature fusion in both local and global levels enable RdNet to interpolate regularly missing traces with relatively high recovered S/N and handle the spatial aliasing problem. In cases of randomly missing traces, RdNet could produce comparable or slightly worse results than the conventional minimum weighted norm inversion, and reliable results could be obtained with less or moderately missing data, e.g., recovered S/N of ~ 40 dB and 30 dB for 10% and 30% randomly missing traces, respectively. Whereas, with the increase of the missing-trace percentage, errors are likely to focus in the area with big data gap (typically larger than five consecutive traces), which could be improved by including more train data for these cases in future work.

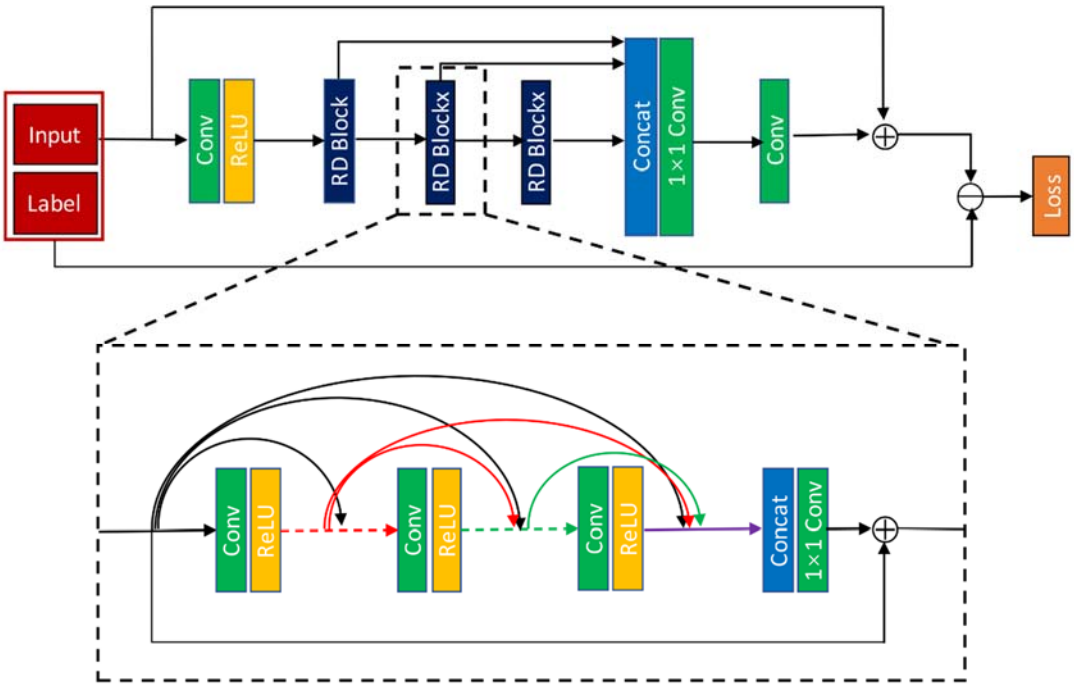

FIG. 1. The architecture of the RdNet used in this study (modified from Zhant et al., 2018).

Theory based machine learning elastic full waveform inversion based on recurrent neural network with various of parameterizations

Tianze Zhang, Kris Innanen, Jian Sun, and Daniel Trad

ABSTRACT

In this study, we combine the recurrent neural network with the knowledge about elastic wave propagation and inversion theory, which forms the theory-based machine learning method for full waveform inversion. Based on the Automatic Differential method, the exact gradient based on the computational graph would be calculated to update the elastic models. To tackle with the cross-talk problem in multiparameter full waveform inversion, we use different parameterizations to mitigate the trade-off issue by modifying the theory-based. RNN cell. From the numerical inversion tests, we can see the different effects on the inversion results with different parameterizations. Different levels of noise have also been added to the observe data to test the performance of this method. This inversion method combines the knowledge we know about wave propagation and inversion theory with the recurrent neural network. It could be the pioneer for us to introduce more complicated theory-based machine learning methods into Geophysics inversion problems.

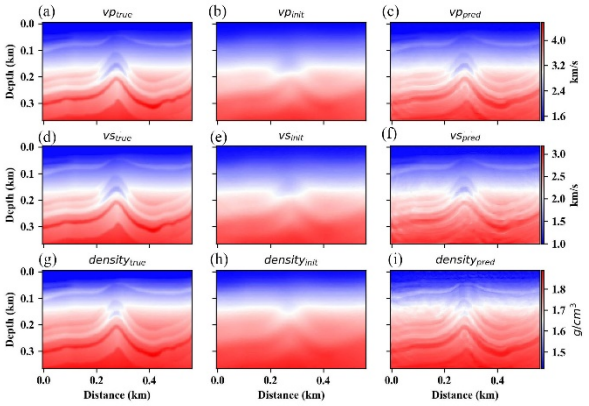

FIG. 1. Velocity parameterization.

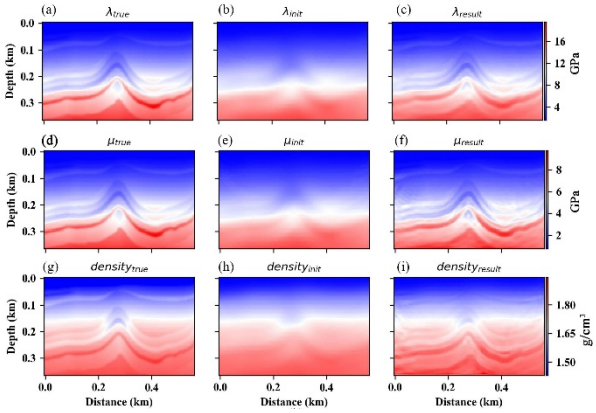

FIG. 2. Modulus parameterization.

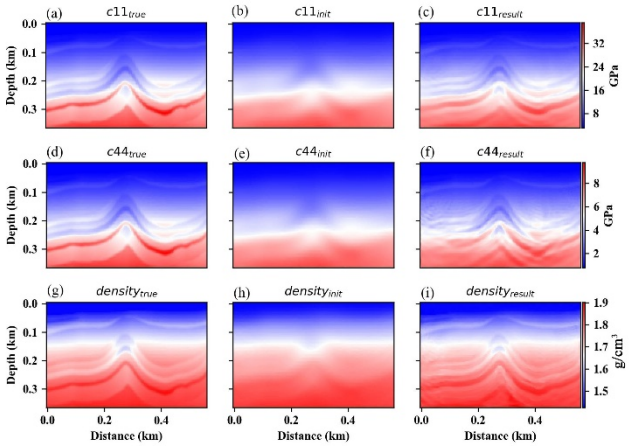

FIG. 3. Stiffness matrix parameterization.

Theory based machine learning viscoelastic full waveform inversion based on recurrent neural network

Tianze Zhang*, Kris Innanen, Jian Sun, and Daniel Trad

ABSTRACT

In this study, we use the recurrent neural network (RNN) to achieve viscoelastic full waveform inversion. The RNN is a typical type of neural network that is consisted of several RNN cells. In this study, each RNN cell is designed according to the stress velocity viscoelastic wave equation. With the Automatic Differential engine built in the machine learning library, the exact gradient for the trainable parameters, the velocity models and attenuation models, would be given based on the computational graph. Both the simple and complex model numerical inversion tests prove that the inversion based on this theory guided recurrent neural network can give accurate inversion results. The performance of this RNN based inversion with different objective functions are also tested. Three objective functions are tested here, which are the l_1 norm, l_2 norm and Huber objective functions. All the three objective functions can provide the right inversion results, however, the l_1 norm and Huber objective function have better accuracy to reconstruct the high wavenumber components of the modes. The l_2 norm inversion has the best data residual convergence rate, but l_1 norm and Huber objective function have better accuracy to reconstruct the models. Compared with Q_p and Q_s, the inversion for V_p, and V_s are more stable with all the three objective functions.

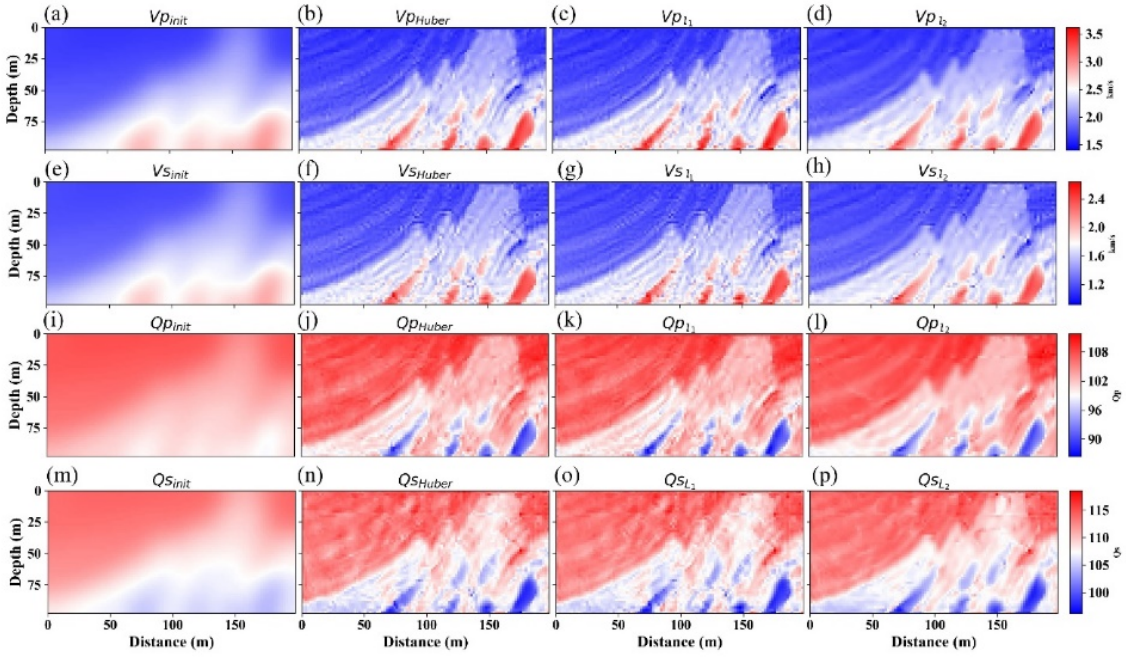

FIG. 1. Viscoelastic RNN inversion results.

Sparse inversion based deblending in CMP domain using Radon operators

Kai Zhuang* and Daniel Trad

ABSTRACT

We implemented a deblending scheme within an inversion-based framework in the CMP domain to test the efficacy of deblending outside the commonly used receiver domain. By operating in the CMP domain instead of the receiver domain, dipping reflectors are centered as opposed to apex shifted, this allows us to implement a simple hyperbolic Radon operator to decrease processing time taken to invert for a deblended data set versus an apex shifted operator. The Radon operator is posed using a $\mathcal{L}_1$ model norm to support focusing in the Radon domain allowing better mapping of data back to their focused gathers. Inversion based deblending is a relatively newer route to exploring deblending, with previous source separation implementations being either denoising the pseudo-deblended data or through windowing in apex shifted radon space. Inversion based deblending allows us to explain all the data by refitting back to the blended dataset using the blending operator.

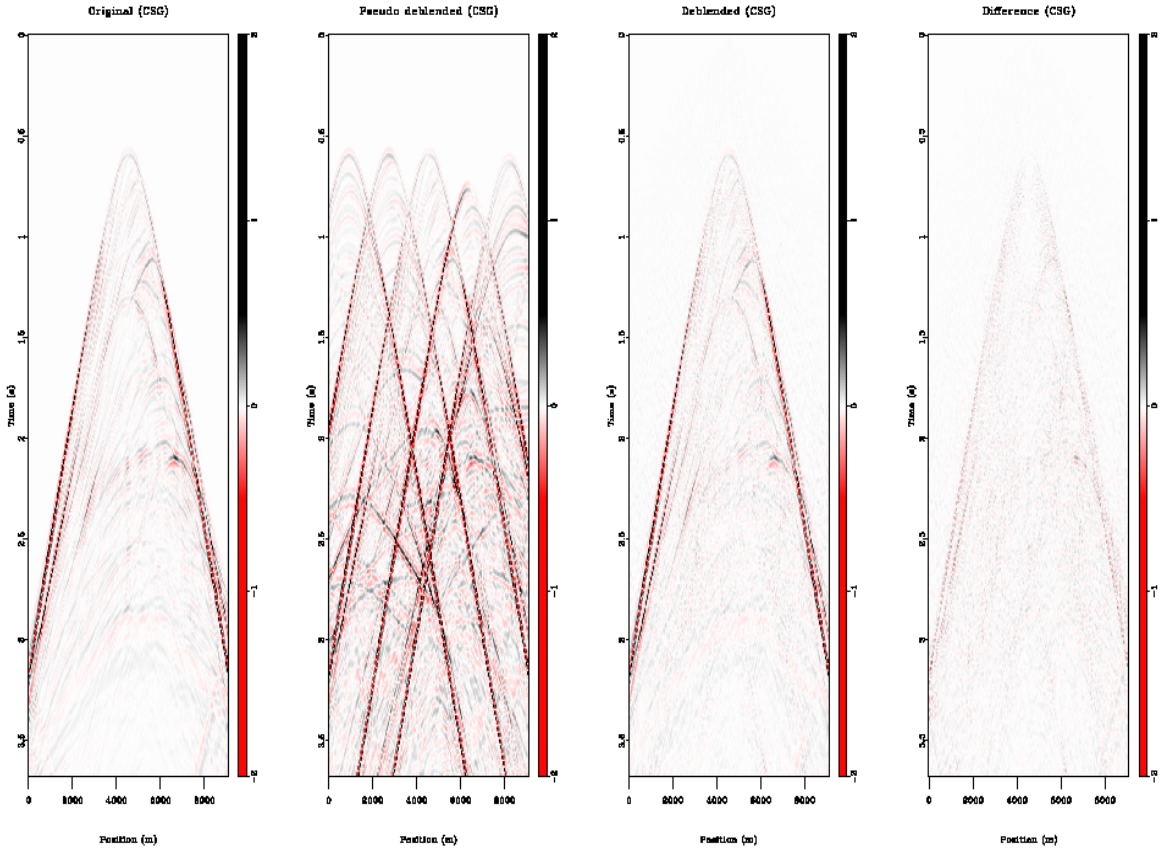

FIG. 1. Deblending the Marmousi model. The Marmousi data with 5 simultaneous shots deblended in the CMP domain and shown in the shot domain, it can be seen that the difference is just amplitude variation and all events are recovered.